

COASTAL EVOLUTION OF A SUBMERGED BRONZE AGE LANDSCAPE AT
PAPADIOKAMPOS, CRETE (GREECE)

A THESIS SUBMITTED TO THE GRADUATE DIVISION OF THE UNIVERSITY OF
HAWAI'I AT MĀNOA IN PARTIAL FULFILLMENT OF THE REQUIREMENTS FOR
THE DEGREE OF

MASTER OF ARTS

IN

GEOGRAPHY

DECEMBER 2013

By

Rhonda R. Suka

Thesis Committee:

Ross Sutherland, Chairperson

Everett Wingert

Floyd McCoy

Keywords: coastal evolution, bathymetric survey, sea level change

ACKNOWLEDGEMENTS

It is with great pride and honor that I extend my gratitude to each person who saw this thesis through to fruition. The expert guidance and intellectual support given so freely by my committee inspired me to achieve things far beyond what I once thought possible. In addition to a superb team of mentors, I am thankful to those who provided funding and additional support to conduct my research overseas.

I am grateful to the College of Arts and Sciences for granting me the Graduate Student Research Award, which allowed me to pursue research in Greece despite the additional expenses involved. In addition, I would like to express my gratitude for the continuous support of the Department of Geography who granted Graduate Student Merit Awards throughout my course of study.

Foremost, I am grateful and indebted to my committee. Each individual contributed a tremendous amount of time, patience and wisdom throughout this process. If I have become a reflection of all that they have invested in me, I cannot fail in my profession or in my everyday actions.

I would like to thank Ross Sutherland, for agreeing to be my Advisor. His bright mind and calm, composed nature never failed to triumph over the uncertainty that I sometimes felt. His attention to detail and precision contributed significantly to the development of those traits in my own work.

My sincere thanks goes out to Ev Wingert, without whom I would not be a Geographer. His generosity and encouragement instilled within me a pride and invincibility that I will carry forward. His sense of adventure and depth of knowledge lent so much to my studies (not to mention all the letters of reference written without complaint). Our traverse surveys through the jungle remain one of my fondest memories.

A heartfelt thanks is also extended to Floyd McCoy, who has been the most positive force in my academic career for more years than I dare to mention. I cannot express enough gratitude for all the doors that have opened for me due to his guidance and encouragement. It has been an honor to have him as my mentor - Σας ευχαριστώ πολύ.

I would like to acknowledge Chrysa Sofianou of the KD ephoreia for her assistance in obtaining permission for the conduct of this research in Greece. I also thank the Institute of Aegean Prehistory (INSTAP) for providing lab space and informative lectures that contributed to

this research. I am grateful to Tom Brogan for his continuing support and interest in the work at Papadiokampos, which allowed me to complete the research at this site.

During this academic journey, I have had the opportunity to expand into acoustic research through work at the Hawaii Experimental and Acoustic Range laboratory. The generous support, patient training and friendship from Eva Marie Nosal and Tom Fedenczuk have sustained me throughout my studies. Their patience and faith in my capabilities speaks highly of their commitment to the success of their students. Under their tutelage, I acquired technical and engineering skills that I have drawn upon many times since.

I would like to thank the people in Greece who helped make this research a success. I am grateful to Elli and Iannous who welcomed me into their home and shared their culture, language, food and friendship.

A loving thank you to my daughters Taylor and Megan and also my partner Gary Baker for all of their patience, encouragement and personal sacrifices they have each made to help me succeed.

I dedicate this work to my late Mother, who would be immensely proud of this accomplishment. Her hard work and ability to overcome obstacles inspired me to be the first ever in our family's history to pursue an advanced degree.

ABSTRACT

The unprecedented changes in climate we are experiencing today drive sea level variations that influence the morphology of coastlines. Many areas experience high rates of sea level rise combined with tectonic movements that abruptly change coastal morphology. One problem with assessing these areas is the lack of data available. Although recent developments have improved our ability to gather information from shallow coastal areas, these systems are expensive and require highly skilled operators and analysts. To alleviate this problem, a portable survey system was developed and tested on the coast of Crete, Greece to determine shoreline changes since the Bronze Age. Results of the survey indicate that the shoreline submerged 10.3 m and moved a minimum of 28 m inland over the past 3463 years. By understanding shoreline change in areas faced with sea level rise compounded by tectonic movement, we can improve our planning and disaster management capabilities.

TABLE OF CONTENTS

ACKNOWLEDGEMENTS	II
ABSTRACT	IV
TABLE OF CONTENTS	V
LIST OF FIGURES	VIII
LIST OF ABBREVIATIONS	X
CHAPTER ONE – INTRODUCTION	1
1.1 NATURE OF THE PROBLEM	1
1.2 STUDY SITE	4
1.3 RESEARCH QUESTIONS	5
1.4 BENEFITS OF THE RESEARCH	6
1.5 STRUCTURE OF THE THESIS	7
CHAPTER TWO - SHORELINE EVOLUTION AND GEOMORPHOLOGY	8
2.1 EUSTATIC SEA LEVEL CHANGE	8
2.2 RELATIVE SEA LEVEL CHANGE	9
2.3 HUMANS AND SEA LEVEL CHANGE	10
2.4 MAPPING COASTAL EVOLUTION	10
CHAPTER THREE - BATHYMETRIC SURVEY FOR RECONSTRUCTING COASTLINES OF THE PAST	13
3.1 SONAR	13
3.2 GLOBAL POSITIONING SYSTEM	15
3.3 IMAGING AND GEO-REFERENCE	16
3.3.1 Remote Sensing	16
3.3.2 Underwater imaging	17
3.4 INSTRUMENT PACKAGE DESIGN FOR SHALLOW WATER SURVEY	18
3.5 SUMMARY	19
CHAPTER FOUR - METHODS	21
4.1 SHALLOW WATER BATHYMETRIC MAPPING	21
4.2 REMOTE SENSING	22
4.2.1 Satellite Images	22
4.2.2 Underwater Photographs	22
4.2.3 Image processing	23
4.2.4 Depth Survey	23
4.3 SUBSTRATE SAMPLING	26
CHAPTER FIVE - CONTOUR AND SUBSTRATE MAPPING	27
5.1 CONTOUR MAPS	28
5.2 SUBSTRATE CLASSIFICATION MAPS	29
6.1 ACCURACY ASSESSMENT OF FIELD DATA COLLECTION AND MAPS	32
6.1.1 Bathymetric (vertical) survey assessment	32
6.1.2 GPS (horizontal) survey assessment	34

6.1.3 Digital Elevation Model accuracy assessment.....	36
6.2 RESEARCH OBJECTIVES	38
6.3 RESEARCH SUMMARY	42
6.4 IMPLICATIONS OF RESEARCH AND FUTURE STUDY	42
APPENDIX.....	44
BIBLIOGRAPHY	61

LIST OF TABLES

TABLE 1. FGDC ACCURACY STANDARDS FOR BATHYMETRIC SURVEYS (FGDC 1998).....	33
TABLE 2. NGS ACCURACY STANDARDS FOR GPS SURVEYS (NGS 1989).	35
TABLE 3. USGS ACCURACY STANDARDS FOR DEMs (USGS 1997).	37
TABLE 4. COEFFICIENTS FOR SOUND VELOCITY UNESCO EQUATION (CHEN AND MILLERO 1977).	45
TABLE 5. ONE MINUTE DEPTH READING AT 1.2 M AND 0.9 M.	49
TABLE 6. ONE SAMPLE ANALYSIS FOR 1.2 M DEPTH.	50
TABLE 7. ONE SAMPLE ANALYSIS FOR 0.9 M DEPTH.	50
TABLE 8. IMPEDENCE OF MATERIALS (LANBO 2006).....	51
TABLE 9. CEMENT AND SAND SUBSTRATE MEASUREMENT COMPARISON AT 1.1 M DEPTH.	52
TABLE 10. ONE SAMPLE ANALYSIS AND PAIRED MEANS COMPARISON TESTS FOR CEMENT AND SAND SUBSTRATE DEPTH MEASUREMENTS. TABLE A7.	53
TABLE 11. ACOUSTIC DEPTH MEASUREMENT WITH A 5 DEGREE AND 10 DEGREE ROLL ANGLE.....	56
TABLE 12. STATISTICAL ANALYSIS OF ACOUSTIC DEPTH MEASUREMENT AT 5 AND 10 DEGREE ROLL ANGLE (RESPECTIVELY).	57

LIST OF FIGURES

FIGURE 1. SEA LEVEL TREND FOR PERIOD 1993-2012. PURPLE COLOR INDICATES A SEA LEVEL INCREASE OF 9 MM/YEAR (NOAA 2013).	2
FIGURE 2. EARTHQUAKE EPICENTER LOCATIONS FOR THE PERIOD 1993-2012 (USGS 2013).....	2
FIGURE 3. STUDY SITE AT PAPADIOKAMPOS, ISLAND OF CRETE, GREECE.....	4
FIGURE 4. DIGITALGLOBE WORLDVIEW 2 SATELLITE IMAGE OF STUDY SITE USING NEW OCEAN BAND SENSOR TECHNOLOGY (DIGITALGLOBE 2011).	17
FIGURE 5. BATHYMETRIC SURVEY INSTRUMENT PACKAGE. FLOATING PLATFORM WITH INTEGRATED SINGLE-BEAM SONAR, NMEA COMPATIBLE GPS UNIT AND SYNCHRONIZED UNDERWATER CAMERA.	19
FIGURE 6. IMAGE CREATED BY LOWERING A CAMERA TO RECORD WAVE CUT NOTCH FEATURE ON A VERTICAL SURFACE.....	22
FIGURE 7. UNDERWATER UNDERCUT AND BROKEN SUBSTRATE ALONG SUBMERGED EROSION EDGE ^(A) AND SUBAERIAL UNDERCUT AND BROKEN SUBSTRATE ALONG SHORELINE WAVE EROSION EDGE ^(B)	23
FIGURE 8. UNDERWATER PHOTOGRAPH MOSAIC OF ROCK CUT AREA CREATED WITH MICROSOFT ICE. HORIZONTAL PLANES ARE AT DIFFERENT LEVELS THROUGHOUT THE AREA. VERTICAL CHANNELS CUT AROUND EACH SLAB ARE UP TO 1.5 M DEEP. SHAPES AND SIZES OF CUT BLOCKS ARE HIGHLY VARIABLE. IT APPEARS THAT THIS AREA WAS ABANDONED OR SUBMERGED BEFORE THE RESOURCE WAS EXHAUSTED.	24
FIGURE 9. SURVEY TRANSECT PATHWAYS.....	25
FIGURE 10. CALCULATED LINEAR COVERAGE OF SONAR BEAM BY DEPTH. (SEE APPENDIX FOR FORMULA.).....	26
FIGURE 11. LOCATION OF GEOLOGIC SAMPLES INDICATED BY YELLOW DOTS.	27
FIGURE 12. CONTOUR MAP OF PAPADIOKAMPOS.....	28
FIGURE 13. CLOSE UP CONTOUR MAP OF WESTERN SIDE OF BAY WITH ARCHAEOLOGICAL SITES INDICATED AS A-D.....	29
FIGURE 14. BATHYMETRIC SUBSTRATE CLASSIFICATION MAP OF PAPADIOKAMPOS BAY. ALL SUBSTRATES THAT ARE UNCLASSIFIED(WHITE) ARE SOLID ROCK.	29
FIGURE 15. CLOSE UP OF SUBSTRATE CLASSIFICATION FOR WESTERN SIDE OF PAPADIOKAMPOS BAY.	30

FIGURE 16. ROCK CUTS IN SCHIST UNDERWATER AT PAPADIOKAMPOS WITH MULTI-LEVEL HORIZONTAL PLANES AND VARIABLE SIZE AND SHAPE BLOCKS SIMILAR TO ANCIENT QUARRIES ON THE ISLAND.....	30
FIGURE 17. SUBAERIAL ROCK CUTS IN LIMESTONE AT AN ANCIENT QUARRY IN WESTERN CRETE. THIS AREA WAS UPLIFTED 9 M AND WOULD HAVE BEEN JUST ABOVE SEA LEVEL PRIOR TO UPLIFT.....	31
FIGURE 18. LINEAR REGRESSION ANALYSIS OF DEM FOR 30 POINTS ACROSS PAPADIOKAMPOS BAY SURVEY AREA.	37
FIGURE 19. SCHIST PAVING STONES AT PAPADIOKAMPOS AND PALAIKASTRO WITH STONE TYPES IDENTICAL TO THOSE AT THE ROCK CUT STONE FOUND UNDERWATER AT PAPADIOKAMPOS. .	38
FIGURE 20. PROJECTED BRONZE AGE SHORELINE WITH MODERN SUBSTRATE FEATURES INDICATED.	41
FIGURE 21. SHALLOW WATER LIMIT TEST TRANSECT FROM 1.5 M TO 0 M.	47
FIGURE 22. SHALLOW WATER LIMIT TEST TRANSECT FROM 0 TO 1.5 M.	48
FIGURE 23. LINEAR COVERAGE OF SONAR AT DEPTHS FROM 1.5 TO 30 M.	55

LIST OF ABBREVIATIONS

ASTER	Advanced Spaceborne Thermal Emission and Reflection Radiometer
BCE	Before Current Era
DEM	Digital Elevation Model
dGPS	Differential Global Positioning System
EGNOS	European Geostationary Navigation Overlay Service
FGDC	Federal Geographic Data Committee
GDEM	Global Digital Elevation Model
GPS	Global Positioning System
IPCC	Intergovernmental Panel on Climate Change
LiDAR	Light Detection and Ranging
NMEA	National Marine Electronics Association
NOAA	National Oceanic and Atmospheric Administration
NSSDA	National Standard for Spatial Data Accuracy
Radar	RADio Detection And Ranging
RMSE	Root Mean Square Error
RTK	Real Time Kinetic
Sonar	SOund Navigation And Ranging
USGS	United States Geological Survey
WAAS	Wide Area Augmentation System

CHAPTER 1. INTRODUCTION

1.1 NATURE OF THE PROBLEM

Shorelines are a dynamic boundary between land and sea. Humans have been drawn to these energetic environments for the wealth of natural resources, potential for commerce, transportation options, favorable climates and natural beauty. Today, nearly 40% of the world's population lives within 100 km of a coastline (UNEP 2012). The growing population density in coastal areas brings an increasing need for understanding coastal change to improve resource management, risk assessment and hazard preparedness.

Today we face unprecedented atmospheric changes that are affecting global sea levels. However, sea level change varies widely across time and space. Changes in coastal morphology have serious consequences for societies and the resources they depend upon. These include erosion and accretion, loss or migration of estuaries, damage to coastal structures, saltwater intrusion and inundation, loss or migration of littoral ecosystems, riverine channel and delta reformation as well as changes in useable land area and associated infrastructures. Two important questions in the study of sea level change today are - how fast will sea level change occur regionally? Moreover, how much land will be lost from these changes? Reconstructing coastal landscapes of the past can provide us with some insight about the changes we might expect today from sea level change, something we must consider in light of the most conservative estimated (RCP 2.6) sea level rise of 0.26 to 0.55 m by the end of the century (IPCC 2013).

To address these questions we need to understand how shorelines respond to two of the main forces that shape them – sea level and vertical tectonic movement. Globally, sea level (Figure 1) and tectonic movement (Figure 2) are highly variable. This emphasizes the need to gain an accurate understanding of how shorelines respond to these forces on a local scale to determine the potential pace and extent of coastal change.

Areas that experience high rates of sea level rise coupled with frequent tectonic movement will experience the most intense shoreline changes. According to data maps generated by the National Oceanic and Atmospheric Administration (NOAA) (2013) and the United States Geological Survey (USGS) (2013) that reflect sea level trends and earthquake epicenter locations, respectively, the areas most affected by these two factors include the islands

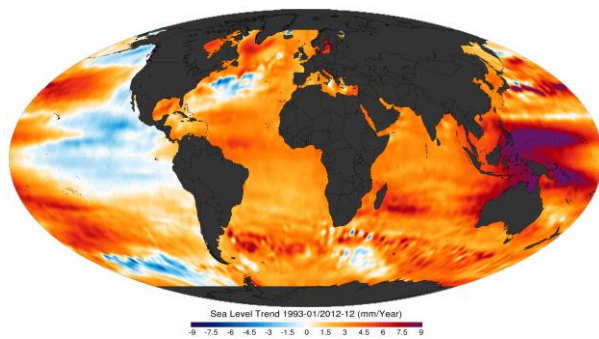


Figure 1. Sea level trend for period 1993-2012. Purple color indicates a sea level increase of 9 mm/year (NOAA 2013).

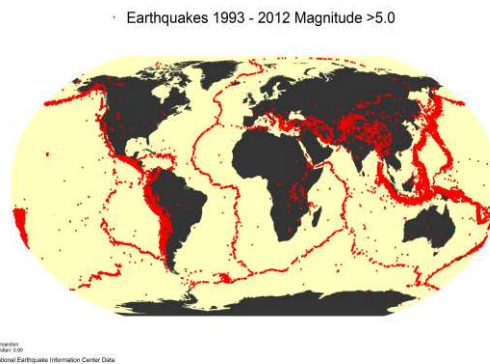


Figure 2. Earthquake epicenter locations for the period 1993-2012 (USGS 2013).

of Melanesia; Indonesia; the Philippines; Japan; the eastern Mediterranean Sea and the southern Kamchatka Peninsula.

The main driver of sea level change today is increased sea surface temperatures, which cause the volume of water to expand resulting in sea level rise. The Mediterranean Sea is particularly sensitive to forces that drive climate change (Giorgi and Piero 2008) and sea level rise (Marcos et al. 2009) because of its geographic characteristics. The Mediterranean Sea is a nearly land-locked, relatively shallow body of water, which has limited circulation and an average tidal range of just 40 cm. These conditions promote surface thermal expansion and accelerate sea level rise. Sea surface temperatures in this area are expected to continue warming and expanding, resulting in a rise of the whole Mediterranean Sea by 3- 61 cm by the end of the century (Marcos and Tsimplis 2008). In one of the most tectonically active places on the planet, these changes will have a dramatic impact on shorelines.

From antiquity, humans have left an archaeological imprint throughout the Mediterranean, providing markers for past sea levels. Areas of long-term occupation are ideal locations to document coastal landscape evolution against a background of human occupation. These long-term records of coastal evolution in the Mediterranean during the Holocene provide insight into the rates of change that impact sea level variation in inhabited coastal areas.

A number of recent studies focus on quantifying sea level change in the Mediterranean (Lambeck 1995, Sivan et al. 2001, Collina-Girard 2002, Lambeck and Purcell 2005, Cundy et al. 2006, Lagares 2007, Scicchitano et al. 2008, Vescogni et al. 2008, Engel et al. 2009, Marcos et al. 2009, Stirling and Andersen 2009, Gehrels 2010, Mourtzas 2010, Shaw et al. 2010, Sivan 2010, Evelpidou et al. 2011a, Goiran et al. 2011, Mourtzas 2012b, Lykousis In Press). These

studies estimate that the rate of sea level rise for the Mediterranean ranges from 3 - 4 m over the past 4000 years.

The submersion of coastal areas in the past throughout the Mediterranean are documented through inference from geologic and archaeological evidence (Sivan et al. 2001, Desruelles et al. 2009, Gaki-Papanastassiou et al. 2009, Anzidei et al. 2011). However, these inferred sea level sequences vary greatly between locations throughout the Mediterranean over the past 6000 years. This variation across a relatively small area emphasizes the importance of gaining an understanding of sea level change on a local scale.

Vertical tectonic movement introduces variations in sea level between closely positioned areas and creates a striking variance across the island of Crete. Records of earthquakes in the past indicate that high levels of tectonic activity are responsible for the main deformation of the island of Crete (tenVeen and Meijer 1998). Coastal morphology has been altered significantly in the past by tectonic uplift of up to 9 m in western Crete (Pirazzoli 2005) and subsidence in central Crete of 1.5 m below modern sea level (Gaki-Papanastassiou et al. 2009). These abrupt changes in relative sea level can cause transgression of the sea up to 78 m inland depending upon the coastal morphology (Mourtzas 2010). Determining the magnitude of tectonic movement helps resolve the temporal pace of sea level change and the implications these movements have on shoreline evolution.

Although a number of investigations have been carried out to identify sea levels of the past in the Mediterranean, few studies have focused on the evolution of the coastline. The data collected for sea level studies is derived from uplifted reefs or archaeological remains on land or in less than 1 m of water, yet many of the coastal landscapes of the past are now in deeper water. The added challenges of collecting data in deeper (>1 m) water has discouraged investigation. Yet, submersion, particularly abrupt submersion such as the neotectonic activity on Crete, often preserves features that are easily destroyed by successive human occupation and subaerial erosion on land and may hold the only evidence remaining of the coastal evolution of an area.

One challenge that impedes work offshore is the lack of a fast, affordable and accurate method for surveying shallow water areas. To address this issue we have developed and field-tested a system that allows quick and efficient data acquisition for these challenging shallow water environments at a low cost. This system is used to collect information about submerged

shorelines and landscape features. The results reveal important insights about how shorelines changed over time and the potential impacts these changes had on ancient coastal settlements.

1.2 STUDY SITE

One area that has the potential to provide a well-preserved record of past submerged landscapes is located on the northeastern shores of the island of Crete in the eastern Mediterranean Sea (Figure 3). The island is located just north of the Hellenic arc, where the African tectonic plate collides and subducts beneath the Eurasian plate.

Major tectonic events of the past are recorded on the west end of the island where ancient shorelines were abruptly lifted 9 m above sea level during 365 AD (Pirazzoli 2005). Evidence for this major event is preserved in the displaced shoreline now positioned on higher ground allowing easy access to the site. Conversely, at the eastern end of the island at Papadiokampos, a Bronze Age (2700 - 1500 BCE) settlement, now partially submerged, indicates that the tectonic movement here is very different from the western end of the island. Subsidence in this area may have preserved features such as drowned waterways, wave-cut notches, rock quarries or other archaeological remains, essentially burying them beneath the water. These features provide insight into the coastal landscape of the past. Because humans have built structures and left their own signature on this landscape for thousands of years, the pace and extent of sea level change and tectonic movement can be measured against a backdrop of human occupation.



Figure 3. Study site at Papadiokampos, Island of Crete, Greece.

1.3 RESEARCH QUESTIONS

Observational records, sea level models and archaeological records provide abundant evidence that coastal areas are vulnerable and strongly impacted by sea level rise, with wide-ranging consequences for human societies and ecosystems. The purpose of this study is to document the landscape imprints of past sea levels on submerged substrates to determine the extent and pace of coastal evolution at Papadiokampos, Crete over the past 4000 years, using modern sea level as a control.

The driving force that has shaped the shoreline is sea level rise. At stable stands of the sea, wave erosion at the shoreline leaves signatures including potholes, sea cliffs, beachrock deposits, wave-cut notches (a concave notch cut into a vertical substrate face), substrate visors (the extended overhang of substrate above a notch) and collapsed overhangs (a visor that is undercut sufficiently to promote collapse).

Vertical tectonic movement also affects shorelines, this intervening variable changes the position of the shoreline relative to sea level. This variable is controlled through known sea levels of the nearest vertically stable coastline located in Israel, where vertical tectonic movement has been less than 0.2 mm/year for the past 8000 years (Sivan et al. 2001). Control for tectonic movement allows separation of this intervening variable from sea level rise.

This research aims to answer the following questions concerning the coastal evolution at Papadiokampos, Crete:

1) **Where was the shoreline during the Bronze Age occupation of this area?**

During the Bronze Age, large coastal settlements were built for the first time on Crete. The remains of these settlements may be observed today on land and offshore. Archaeological evidence (a rock quarry) from this era may provide a limiting value for sea level stands during their time of use.

- Hypothesis 1: If Bronze Age subaerial coastal quarries are now submerged, then sea level was a minimum of 0.60 m below the lowest rock quarry level during the time of use (Anzidei et al. 2011).

2) **What was the spatial sequence of coastal change at Papadiokampos?**

Wave-cut notches indicate the position of mean sea level (Kershaw and Guo 2001, Stewart and Morhange 2009) Wave-cut notches are formed when waves carve laterally into the substrate during sequences of sustained erosion (Cooper et al. 2007). A sequence of wave-cut notches provides an opportunity to locate the position of past sea level and measure the horizontal distance between notches to determine the spatial migration of the shoreline.

- Hypothesis 2: If a sequence of wave-cut notches is now submerged, positions for past shorelines can be determined and the distance between each sea level stand will provide a measurement of transgression between pauses in sea level.

3) **How quickly did shoreline changes occur since the Bronze Age?**

A preserved wave-cut notch (Rust and Kershaw 2000) or archaeological feature (Sivan et al. 2001) indicates removal from a high energy environment caused by an abrupt change in sea level or vertical tectonic displacement. At sites that are exposed to high wave energy, such as headlands, where erosion rates are high, slow changes in sea level can obliterate past erosion signatures. Submersion, as well as uplift, removes sea level indicators from high energy areas preserving a marker of past sea level. The date of submerged artifacts such as coastal quarry work can be inferred by matching quarry stone to archaeological structures on shore (Soles 1983, MacGillivray et al. 1984),(MacGillivray et al. 1984) and provide an inferred sea level (Sivan et al. 2001, Scicchitano et al. 2008).

- Hypothesis 3: If datable material is associated with submerged shoreline features then the historical pace of shoreline change can be determined.

1.4 BENEFITS OF THE RESEARCH

This research will provide archaeologists and geologists with information about the extent of the Bronze Age settlement at Papadiokampos beyond the modern shoreline and the location of significant coastal features such as harbors and quarries, which are poorly documented and understood for this era. Because this particular settlement was abandoned during the Bronze Age for unknown reasons, understanding the pace and extent of shoreline change may also provide archaeologists with some insight about the abandonment of the area.

On a broader scale, the contribution of high-resolution data that documents the extent and pace of sea level change, including vertical tectonic movement and rates of tectonism, benefits predictive modeling efforts. On a local scale, understanding the pace of coastal change, resulting from rapid tectonic shifts or relatively slower sea level rise, is critical for improving hazard prediction and society responses. Improvements can then be made in safe building and development practices, especially in areas that experience accelerated sea level rise combined with tectonic movement.

In addition, bathymetric research will benefit from the development of a fast affordable and accurate method for shallow water surveys. For the first time, investigators will be able to collect integrated depth, position, sample and image data in shallow water areas for a fraction of what it has cost in the past. The methods and instrumentation package that we have developed will make shallow water surveys accessible to multiple fields of research.

1.5 STRUCTURE OF THE THESIS

This thesis contains six chapters. The introductory chapter is followed by Chapter 2, which describes the number of forces that contribute to shoreline change and presents the theoretical base for this study. Chapter 3 discusses bathymetric survey instrumentation and theory as it relates to the reproduction of shoreline evolution. Chapter 4 discusses the research methods and provides a detailed description of the study site. Chapter 5 presents the results of the research effort and addresses the research questions. Chapter 6 discusses conclusions of this research and presents the benefits of this research that are relevant to coastal evolution reconstruction. Future research direction and focus in this area concludes this chapter.

CHAPTER 2. SHORELINE EVOLUTION AND GEOMORPHOLOGY

Sea level is a dynamic force acting upon the coastal landscape, varying in sign and intensity across the globe. Observed variations in sea level rise in major ocean basins (Pacific, Arctic, Atlantic and Indian) show that ocean density and circulation patterns have a significant effect on the amount of sea level change occurring (White et al. 2005). While land-locked seas like the Mediterranean also exhibit a response to these eustatic sea level trends (Cazenave et al. 2001), it is the relative sea level changes that have the most long-term impact on Mediterranean shorelines. This chapter presents the two main forces that contribute to coastal change in the Mediterranean - isostatic adjustment and vertical tectonic movement. These two forces have different effects on any given geographic area. The differences between areas are well illustrated by estimates of Bronze Age sea levels around the island of Crete - north of the island in the southern Aegean Sea, sea level was 3 m below modern levels (Lambeck 1995) and to the east, in the Levantine Basin, sea level was 1.5 m below present levels (Lambeck and Purcell 2005). The impact of rising sea levels on the human population on Crete following the Bronze Age is discussed. This discussion brings us to the end of the chapter where the importance of mapping the spatial and temporal sequence of sea level change is highlighted.

2.1 EUSTATIC SEA LEVEL CHANGE

Eustatic sea level change (ocean volume) is comprised of three main processes – steric expansion or contraction of surface water from temperature or density variations (Wigley and Raper 1987); glacio-eustasy, which is the variation in land ice volume and meltwater contribution to the ocean (Peltier 1999); and tectono-eustasy, which is the variability of ocean basin volume (Rona 1995). Steric sea level rise occurs when temperatures increase and the surface of the ocean warms and expands increasing the space that water is occupying. Glacio-eustasy, also triggered by warmer temperatures, is the contribution of glacial meltwater to the ocean, which increases the total volume of water. When additional water is added to the ocean, the additional weight pushes the sea floor down into the mantle causing bordering continental landmasses to uplift. This process is called continental levering and is associated with tectono-eustasy, which is the crustal response to land ice loads and tectonics (Mitrovica and Peltier

1991). Land ice distributes a heavy load onto the underlying land surface, when the ice melts, the load is relieved and the underlying surface of the land rebounds. This rebound pulls plastic mantle material in from the surrounding area to fill the expanding space. This rebound response causes uplift in ice-free areas and subsidence in the surrounding sea floor, enlarging the volume of the ocean basin.

These variations in eustatic sea level are pronounced today in the relatively shallow, nearly enclosed Mediterranean basin where evaporation outpaces precipitation and input from terrestrial waterways and limited circulation raises the water density allowing surface water to warm and expand. These conditions combine to produce large variations across the Mediterranean basin, with the largest sea level increases, >30 mm/year, in the eastern portion southeast of the island of Crete (Cazenave et al. 2001).

2.2 RELATIVE SEA LEVEL CHANGE

Relative sea level change is a regional process that is associated with land movement relative to sea level. There are several forcing agents for relative sea level – ocean dynamics (El Nino/La Nina events, ocean currents, Pacific Decadal Oscillation, North Atlantic Oscillation and geostrophic forces), gravitational variance, subsidence from groundwater removal, tectonic movement (subsidence or uplift), sedimentation and erosion, hydro-isostasy (ocean basin sinking) and glacio-isostasy (land rebound after deglaciation). These processes vary considerably by region and add complexity when contributed to the Mediterranean sea level curve. The two dominant relative sea level forces in the Mediterranean, tectonic movement and isostatic adjustment, are the focus of this discussion.

Since the last glacial maximum, isostatic adjustments have had dominating influences on sea levels in the Mediterranean (Lambeck and Purcell 2005), including seafloor subsidence due to increased water loads and seafloor uplift or subsidence due to isostatic adjustment of the earth's crust in response to shifting surface loads.

Tectonic events cause abrupt changes in relative sea level that have major impacts on the evolution of coastal landscapes. At convergent and divergent plate boundaries, vertical tectonic movement displaces shorelines in abrupt and sometimes catastrophic events creating uplift or subsidence of the land, intensifying coastal change. It is important to separate the movement

associated with vertical tectonic activity from eustatic changes in sea level (Woodworth and Player 2003). Regional variations highlight the need to understand how sea level change affects coastal evolution, especially at converging plate boundaries with frequent tectonic activity.

2.3 HUMANS AND SEA LEVEL CHANGE

Long-term records of coastal evolution in the Mediterranean area during the Holocene provide an indication of the impact of sea level change. From antiquity, humans have left a cultural imprint, providing markers for past sea levels. Areas of long-term occupation are ideal locations to document coastal landscape evolution against a background of human occupation. The changes that take place within a human timeframe provide insight into the impact these changes have on societies and the resources of inhabited areas. Cultural deposits also provide an opportunity to assign a date for changes in coastal environments.

Changes in coastal morphology from sea level rise causes inundation in low-lying areas, where humans often live, breakwaters are submerged leaving harbors unprotected, coastal roads and harbor structures are inundated impeding trade, fresh water stores are compromised by saltwater intrusion and coastal natural resources are damaged. Low-lying areas on land adjacent to the sea are in a higher energy zone and as such are more vulnerable to changes in sea level and further shoreline transgression. The transgression of sea level across a coastal area on Delos Island north of Crete submerged a 30 m swath of ancient landscape, radically altering the morphology of the coastline (Mourtzas 2012b). Abrupt changes in sea level due to tectonic movement are particularly devastating. A long-term view of coastal response to sea level change on a local scale is imperative for us to understand, especially during periods that humans have responded to these agents. This information allows us to evaluate modern coastal vulnerability, catastrophic response scenarios and adaptation strategies.

2.4 MAPPING COASTAL EVOLUTION

Sea level markers must be identified and dated to determine the evolution of a shoreline. Often sea level markers are submerged. The information contained in these submerged landscapes cannot be captured using terrestrial surveys. Even the most sophisticated remote

sensing, including Light Detection And Ranging (LiDAR) which analyses laser light reflectance of a surface to determine elevation and RAdio Detection And Ranging (RADAR) which determines elevation through analysis of radio wave energy returns from a surface, cannot identify these submerged markers. Bathymetric surveys provide the highest resolution method today for identifying and documenting the position of submerged sea level markers. Submersion often preserves shoreline features (Boulton and Stewart 2011) that would have been destroyed by successive human occupation or subaerial erosion on land and may hold the only evidence remaining of the coastal evolution. One thing that hampers bathymetric survey work is the lack of an easy to use, fast, affordable and accurate method for surveying shallow water areas. One goal of this project is to develop and field test a system that allows quick, efficient and cost effective data acquisition for this challenging environment.

Determining the spatial rate of coastal change allows measurement of land loss and can indicate the rate of coastline change. To gauge the spatial rate of sea level change, archaeological and geologic markers are the best inferences on a local scale in the Mediterranean (Lambeck 1995). In many locations throughout the Mediterranean, archaeological and geologic markers are submerged and the spatial sequence of coastal evolution can only be determined through bathymetric survey.

The position of archaeological structures which have an elevation relative to sea level at their time of use such as structural floors and coastal quarries that require a minimum elevation above sea level to be in effective use, are reliable indicators of sea level (Anzidei et al. 2011). Mapping the position of these structures in relation to modern sea level allows us to infer the vertical sea level change since their time of use.

The temporal sequence of coastal evolution in the Mediterranean is more challenging to determine due to the lack of commonly used markers such as coral and salt-marsh environments that may be cored and dated. However, the advantage of studying the Mediterranean environment is the long history of human occupation that left behind a well-documented archaeological record. This archaeological record provides an established timeframe for artifacts. The position of archaeological structures that are more resilient in submerged environments can provide a datable sequence for relative sea level.

Geologic markers of sea level include beachrock formations and wave-cut notches. These markers indicate the position of past shorelines. In the Western Mediterranean, a

sequence of wave-cut notches between 0 and 60 m reveal a sequence of Late Quaternary sea level change (Collina-Girard 2002, Rovere et al. 2011).

Geological markers like beachrock can also provide a temporal sequence. Beachrock forms in the intertidal zone under stable sea level conditions where sedimentary material cements into benches of rock. The diagenetic cement that forms between sand grains in beachrock in the intertidal zone during periods of sea level stability can be radiocarbon dated (Desruelles et al. 2009). Although the dating of beachrock through ^{14}C methods may slightly overestimate the age of formation, beachrock is often the only existing temporal marker available in submerged environments. Biological markers are often incorporated into these marine substrates and provide another material that can be dated. The remains of carbonate secretions from boring invertebrates that inhabit a narrow range below the sea surface within the intertidal and immediate subtidal zone offer an opportunity to obtain a radiocarbon date for past sea level. These dates allow the assignment of an age for the intertidal phase of the substrate.

CHAPTER 3.

BATHYMETRIC SURVEY FOR RECONSTRUCTING COASTLINES OF THE PAST

This chapter presents the bathymetric survey theory of shallow near-shore areas. A description of appropriate Sound Navigation And Ranging (SONAR) and Global Positioning System (GPS) instrumentation for bathymetric survey use is followed by a discussion of the imaging technology that compliments bathymetric surveys. The development of an instrument platform that meets the environmental demands of a bathymetric survey effort at Papadiokampos is presented. The conclusion of this chapter highlights the limitations and accuracy of the proposed survey system.

3.1 SONAR

Surveying an underwater landscape involves some unique challenges. Wave energy, turbidity, currents and exposure to harsh environmental conditions often prevent the collection of quality bathymetric data. Shallow water, shoals and obscured outcrops often prohibit vessel access. However, when conditions allow, a bathymetric survey can produce valuable information about the coastal environment. Bathymetric surveys incorporate a variety of instruments to determine the depth, position and shape of features on the sea floor. The use of sonar is well suited for large areas to identify points of interest (Rovere et al. 2011) or to obtain bathymetric profiles (Evelpidou et al. 2011b).

Sonar instruments determine depth from an acoustic signal. A directional signal is emitted from the instrument and reflects off the closest object encountered, usually the sea floor, then returns to the instrument. The time delay between departure and arrival of the signal at the instrument is recorded as depth.

A multitude of sonar instruments are available for bathymetric surveys. These range from vessel mounted instruments that weigh over 100 kg, to small hand-held instruments that a SCUBA diver could use. A single-beam sonar sends out one acoustic signal in one direction at a set rate to record depth or seafloor bathymetry (Kenny and Sotheran 2013). A multi-beam or side-scan sonar instrument sends out multiple, simultaneous signals along a horizontal or angled

swath and records each return independently. This increases the number of data points collected and produces high resolution seafloor data (Smith and Rumohr 2013).

The frequency and beam angle of the acoustic signal determines the optimal depth range for the instrument. Lower frequency (<100 kHz) allows better penetration of the water column with less scattering of the signal. Higher frequencies (>100 kHz) attenuate more quickly but allow higher resolution. Wide beam angles capture a larger area but may lower resolution in deeper water as the beam will cover an even wider area at depth. Narrow beam angles focus on smaller areas of the sea floor and provide higher resolution in deep water. Lower frequency sonar instruments are well suited for shallow water (<30 m) bathymetric surveys because signal strength is strong. A narrow beam angle is also suited for shallow water reducing overlapping point collection and concentrating the signal directly below the instrument for higher accuracy position data (Freitas et al. 2008).

Multi-beam sonar instruments are commonly used in bathymetric survey. These instruments are mounted on a ship's hull or towed behind a ship. The side-scan sonar beam is directed to the side of the ship recording vertical anomalies on the sea floor such as shipwrecks and sea mounts. However, side-scan sonar is not appropriate for determining depth. To determine depth, a multi-beam sonar is used. A multi-beam sonar is aimed down along a horizontal plane and records the depth along a swath of the sea floor as the ship travels forward. These instruments require a computing system and a steady power supply which requires the use of a ship. Although these instruments have high resolution, they are often cost prohibitive and require a dry platform for operation, generally a boat, which inhibits surveys in shallow near-shore areas due to sea floor hazards (Basu and Saxena 1999). This produces a gap in bathymetric data between the shoreline and the minimum depth range of survey vessels. Although LiDAR technology can now provide depth information for this zone, the technology is limited by water clarity and surface turbulence (Guenther 2007). In addition, the limited availability of systems like LiDAR in remote international locations, as well as the associated costs of airborne surveys, often prohibit these surveys of shallow water environments (Guenther et al. 2000).

Since the 1930's, single beam sonars have been used to conduct bathymetric surveys. A single beam sonar provides points of depth data from the sea floor along the path of travel. These systems are smaller, require very little power or electronic support and can be mounted on

virtually anything that floats, allowing more versatility in “vessel” choice, including kayaks, or paddle boards. Although these systems provide details along a narrow swath compared to multi-beam systems, they are well suited for areas that are difficult or dangerous to navigate with a larger vessel and can provide high-resolution data in water depths less than 10 m.

3.2 GLOBAL POSITIONING SYSTEM

Sonar instruments are coupled with GPS units that automatically record position information for each depth point, allowing rapid data acquisition. Standard GPS, Real Time Kinetic (RTK) and Differential Global Positioning System (dGPS) are the three main types of positioning systems used today.

Standard GPS units rely on information contained within the satellite signal instead of the time lapse of the return signal and are corrected through the Wide Area Augmentation System (WAAS) or European Geostationary Navigation Overlay Service (EGNOS). The WAAS and EGNOS correction is determined by satellite base stations in geostationary orbit that calculate the relative position of signal transmitting satellites and relays the correction to receivers continually. Standard GPS units are in wide use today for a variety of purposes. These units provide position accuracy on the order of 5-10 m and are relatively inexpensive.

RTK systems are commonly used in land and hydrographic survey applications. These systems measure the phase of the carrier signal from a satellite-based positioning system to correct the signal. This measurement relies on a single reference station to correct positioning in real time. Distance to the satellite system is measured by time delay of the signal and produces accuracy to within 3 m. Military grade RTK are accurate to within 30 cm or better but signals are encrypted and not available for civilian use. The RTK system requires a base station to relay the corrected signal to multiple mobile units that determine positioning by comparing to the corrected relay signal. The mobile units are then able to correct their position to within 2 cm (Rizos and Han 2003). These units are the most accurate but significantly more expensive than standard GPS units.

dGPS systems are commonly used for navigation purposes and use a network of base stations that collect satellite pseudo-ranges to calculate corrections that are continuously broadcast to dGPS receivers. Receivers must be close enough to the base station to apply the

corrected signal for positioning. The further the receiver is from the base station the less accurate the correction becomes (0.22 to 0.67 m per 100 km). The best horizontal accuracies achievable using dGPS systems are within 10 cm. These units provide lower accuracy but also have a lower cost than RTK units (Norris et al. 1997).

The accuracy of all GPS units are affected by disruptions in the received signal including atmospheric disturbance, physical barriers or reflection (overhead canopy, buildings, mountain ranges, etc.), the number of satellites in view of the receiver, relative position of satellites and satellite signal errors (Andersen et al. 2009).

In remote, isolated areas access to relay stations are often limited or non-existent and multiple GPS units may not be cost effective. The portability and small size of standard GPS units makes them attractive for use in shallow water surveys where a vessel is not practical. The lower accuracy of these units is appropriate for the documentation of sea floor features, as opposed to the need for high precision capabilities required for surveying property boundaries or engineering projects.

3.3 IMAGING AND GEO-REFERENCE

An image record of the sea floor is often necessary for a visual reference and to record highly detailed information that is not captured with sonar data. A wide variety of cameras and remote sensing options are available that allow selection of the most appropriate imaging needed for the survey conditions and limitations expected.

3.3.1 Remote Sensing

On land, topographic maps and aerial photographs provide elevation and landscape feature information. The accuracy of this information can be confirmed through ground inspection of the site (Gaki-Papanastassiou et al. 2009). Geologic and geomorphic category maps may also reveal older landscape features that remain within the landscape. These references are useful in land-based applications but provide little information for underwater areas. Maritime navigation maps that illustrate bathymetry are the best source of information for offshore applications. However, shallow near-shore areas generally have poor feature details due to limited boat access. Satellite imaging detects features visible on the sea floor up to 10 m deep

in calm, clear water and provides latitude and longitude positioning of features. However, these images are not yet able to provide depth information.

To gather preliminary information on the near-shore features at Papadiokampos to prepare for field surveys, an image was procured from DigitalGlobe's World-View 2 satellite. This satellite uses an ocean band sensor that can detect features visible on the sea floor up to 10 m deep in calm, clear water and provide latitude and longitude positioning of features (Figure 4). The images provided for the study site at Papadiokampos were used to determine areas underwater that might have preserved features like wave-cut notches or archaeological structures. These images, combined with maritime maps and terrestrial topographic maps provided a foundation for displaying and analyzing the bathymetric data collected in the field.

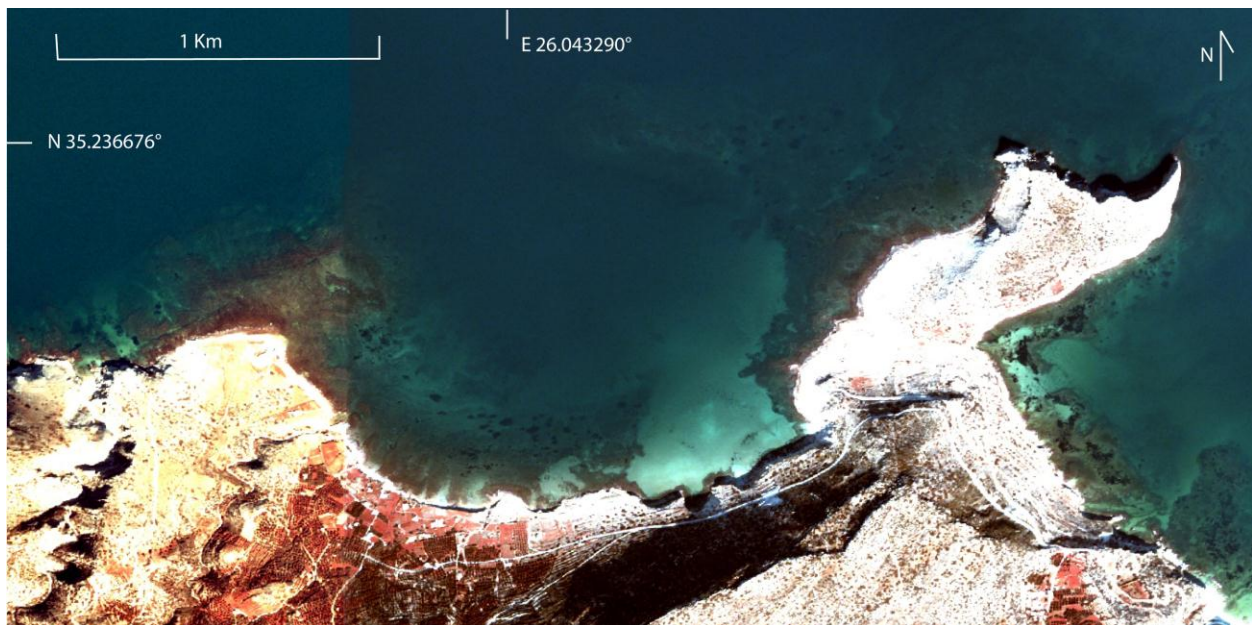


Figure 4. DigitalGlobe WorldView 2 satellite image of study site using new ocean band sensor technology (DigitalGlobe 2011).

3.3.2 Underwater imaging

Digital underwater cameras allow thousands of images to be collected at a minimal cost. One of the smallest and most versatile systems widely available today is a compact, lightweight, waterproof camera called the GoPro HeroCam that can record images automatically at pre-selected time intervals and has High Definition video capability. Using this camera, we were

able to synchronize the photographic time interval with the sonar and GPS units to provide geo-referenced images of the sea floor.

3.4 INSTRUMENT PACKAGE DESIGN FOR SHALLOW WATER SURVEY

To survey the shallow near-shore area at Papadiokampos, we designed an instrument package that integrates a NMEA 0183 compatible GPS unit with a single beam sonar sampling at 160 kHz, and an underwater camera (Figure 5). The instrument provides position, depth and image data at a pre-selected automatic sampling rate from a small floating platform navigated by a swimmer. The instrument package is powered by 8 standard D-Cell batteries that are housed in a watertight transparent box with the GPS unit. Data cables allow the GPS to synchronize position data with depth information from the sonar instrument at 5 s intervals. The underwater camera is set to capture an image every 5 s in synch with the GPS and sonar data collection. The 5 s interval was selected to allow the greatest data collection within the limits of the battery and media card capacity. In addition, in a 5 s interval the operator swims 20 m. This distance is beyond the horizontal error of the GPS unit thus reduces the possibility of overlapping GPS positions.

The benefits of this system set-up are the portability, reduced initial and operational cost and the large volume of data collection possible within a short time period. An added benefit is that the unit is operated by a swimmer with a continuous view of the seafloor through a dive mask. This allows features of interest to be targeted and surveyed in more detail allowing streamlining of data collection.

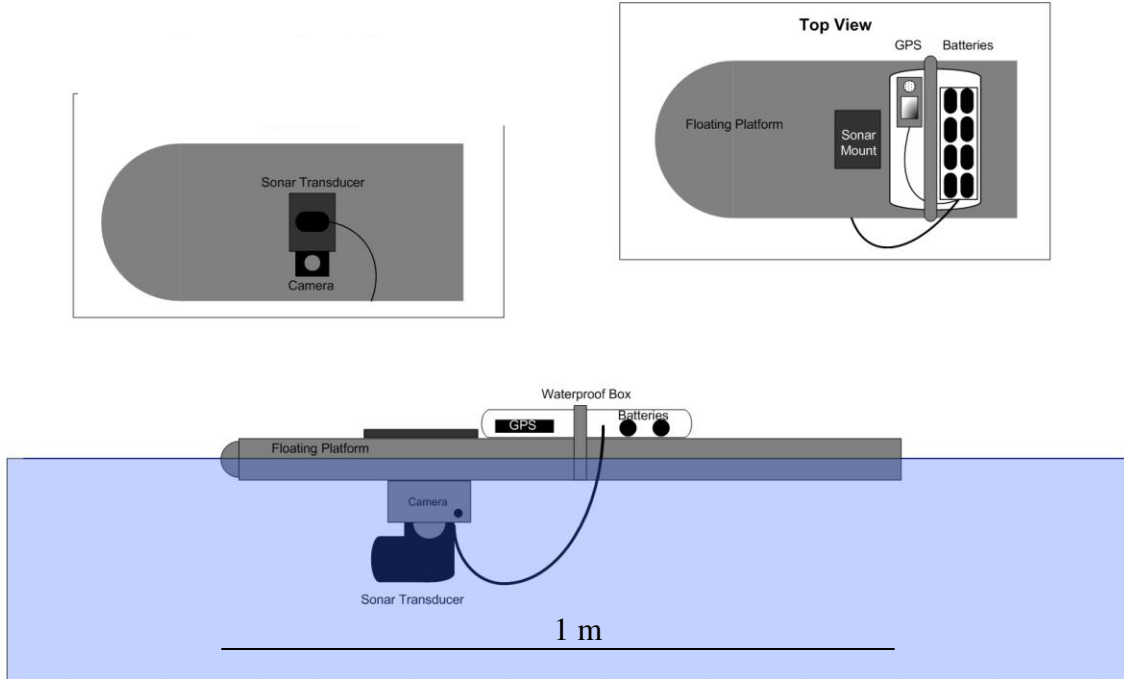


Figure 5. Bathymetric survey instrument package. Floating platform with integrated single-beam sonar, NMEA compatible GPS unit and synchronized underwater camera.

Each instrument in this system has limitations that are quantified through manufacturer specifications or through our own field-testing. These specifications and limitations are detailed in the Appendix.

Shallow water bathymetric surveys in remote areas require a fast, affordable and accurate methodology. With the development of this instrument package, investigators will now be able to collect integrated depth, position, sample and image data for shallow water areas for a fraction of the time and cost. The method and instrumentation package that we have developed will make shallow water surveys accessible to multiple fields of research that can be carried out virtually anywhere that it is safe to swim.

3.5 SUMMARY

This survey system design is easily transported and deployed by a single person and collects data efficiently at high resolution at a minimal cost. Overall, the speed and low cost of this system makes it an attractive option for remote areas that require baseline or repeated

monitoring. The system would also perform well in relatively calm water environments such as estuaries, lakes and lagoons to measure bathymetric changes due to sea level changes, silting or catastrophic events.

CHAPTER 4. METHODS

Our portable survey system was designed to meet the research requirements for surveying the sea floor along a remote section of the eastern coast of Crete, Greece where excavations on shore have revealed a Bronze Age settlement that is now partially underwater. The primary function of the survey system is to collect bathymetric data to document former shoreline features now submerged and possibly human made artifacts. A secondary function of the system is to collect image data so that details of features are recorded and any archaeological finds can be reported to the excavation team on shore. The environmental conditions, as well as time and cost constraints, demanded a system design that could be easily deployed by one or two people that could be transported easily across rugged terrain and collect data quickly from a small floating platform. We also designed a methodology to compliment the survey system that allowed collection of ancillary seafloor data.

This chapter details the methodology used in the field to collect georeferenced data of seafloor features. The methods used to collect supporting data that provide geologic and surface feature information of the sea floor are also discussed. The mapping techniques used to compile and analyze the collected data are presented. The methods used to produce bathymetric profile maps are detailed as well. To conclude this chapter, an accuracy assessment of the field data collection and mapping are outlined.

4.1 SHALLOW WATER BATHYMETRIC MAPPING

There are a number of different methods and instrumentation used to produce bathymetric maps. A careful selection of tools and instruments is required to produce a map with sufficient detail of the sea floor to determine coastal evolution. The research presented here uses photo interpretation of remotely sensed images and interactive digitizing mapping methods. Interactive digitizing allows the use of photographs or satellite images as a base to add polygons or other information to build a complete map. To provide detail in the bathymetric map all images collected in the field were georeferenced. The georeferenced images were then used as a reference to identify and characterize morphologically significant features of the sea floor.

4.2 REMOTE SENSING

4.2.1 Satellite Images

The Digital Globe World-View 2 satellite images were used to detect major underwater features underwater. These images combined with terrestrial topographic maps provided a reference foundation for interactive digitizing of bathymetric field data. These images do not provide water depth information but provide a geo-referenced image base for depth data to be displayed using ArcGIS software.

4.2.2 Underwater Photographs

To determine the identity of features visible in the satellite images and also to record more detail of the seafloor surface, we used a small sport camera in an underwater housing. A GoPro HeroCam was mounted to the bottom of the floating survey platform and synchronized with the GPS unit to capture an image every 5 s. The time stamp on both instruments allows assignment of a geo-referenced position for



Figure 6. Image created by lowering a camera to record wave cut notch feature on a vertical surface.

each photograph. From these images, a detailed classification of seafloor characteristics for a given area were created, such as the location and extent of seagrass beds, sand fields, loose rock accumulations, solid substrate and relict channel formations. This allowed the delineation of areas with homogenous characteristics to be classified and plotted for analysis in ArcGIS.

Areas with vertical relief such as cliff faces are not captured well from a surface-down view. To record these features, a second camera lowered down to the feature depth was used to collect supplementary oblique angle images. To collect a sequence of photographs, the camera was set to record an image every second and maneuvered to the seafloor feature using two ropes guided by a swimmer at the surface. This technique allowed collection of georeferenced images without requiring the swimmer to repeatedly dive to depth. This method also allowed images of features beyond free diving depth range to be collected with ease, providing a multitude of images for each feature (Figure 6).

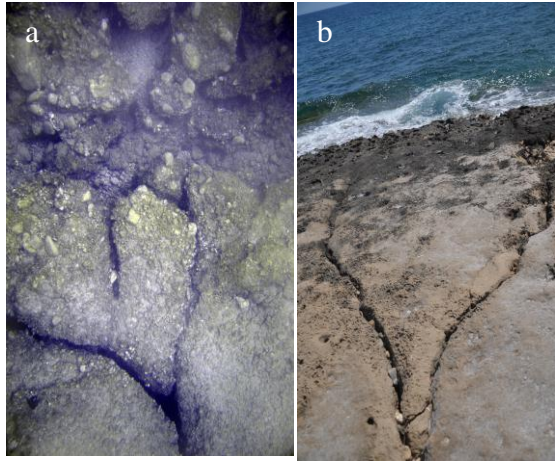


Figure 7. Underwater undercut and broken substrate along submerged erosion edge^(a) and subaerial undercut and broken substrate along shoreline wave erosion edge^(b).

white, gray or black objects on the sea floor such as rocks or shells. Brightness and contrast levels were adjusted as needed to sharpen images.

After these corrections, a number of images with highly detail features from the rock cut areas, were compiled into a photo mosaic using Microsoft Image Composite Editor (ICE) software. The result is a larger detailed view of the feature, which cannot be captured in a single photo (Figure 8).

4.2.4 Depth Survey

A single beam sonar was employed to record water depths along pre-determined transect paths. Transects were concentrated in the shallow (<10 m) near-shore areas adjacent to archaeological excavations on-shore to increase the probability of recording any human artifacts remaining within the landscape features. Due to a lack of datable material available from the sea floor, human made features may be the only means to determine the temporal sequence of shoreline change in this area. Survey transects were aligned perpendicular to shore from ~1 m depth to at least the 10 m isobath. Conducting surveys perpendicular to shore is more accurate than a random pattern survey with the same data density for a coastal environment because more variation exists in the cross-shore substrate than the along-shore substrate. Four transects spanned the width of the bay, and two transects extended from shore to the 30 m isobath to provide general depth information for the central bay. A series of transects were conducted

A Nikon D70 digital single lens reflex (DSLR) camera was used to collect reference images of subaerial shoreline composition and geomorphology. These images were compared to underwater images to aid in identifying submerged shoreline features (Figure 7).

4.2.3 Image processing

To improve image quality, each underwater photograph was post-processed using Adobe Photoshop Elements 4.0 software. White balance was adjusted for color correction using existing

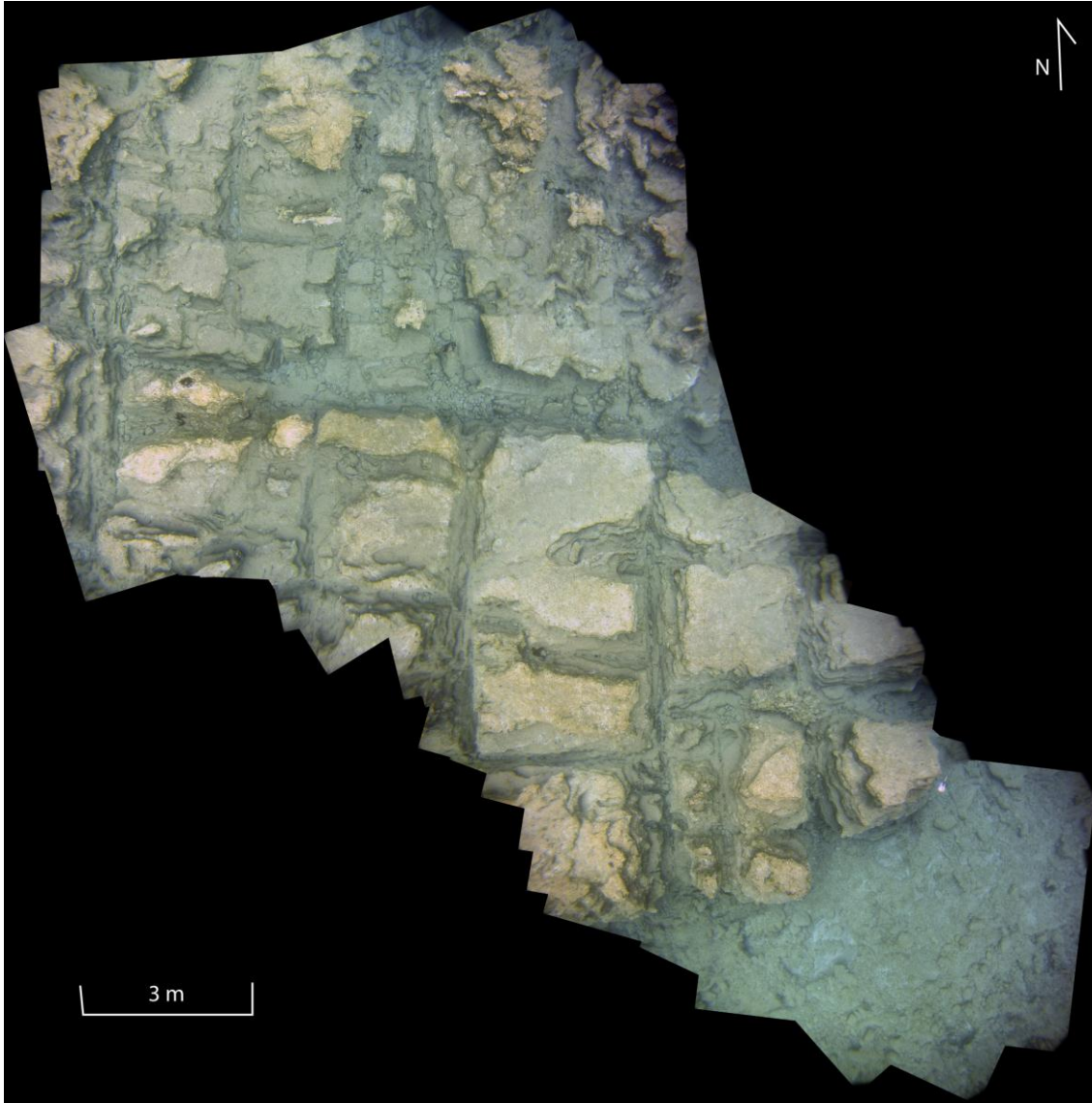


Figure 8. Underwater photograph mosaic of rock cut area created with Microsoft ICE. Horizontal planes are at different levels throughout the area. Vertical channels cut around each slab are up to 1.5 m deep. Shapes and sizes of cut blocks are highly variable. It appears that this area was abandoned or submerged before the resource was exhausted.

parallel to shore across a submerged peninsula that extends from the western headland of the bay (Figure 9). Each transect or series of transects began and ended at an established benchmark on shore with a known location to calculate errors in position fixes during the transect period due to satellite movements. Each transect was corrected for transducer draft and tidal fluctuations.

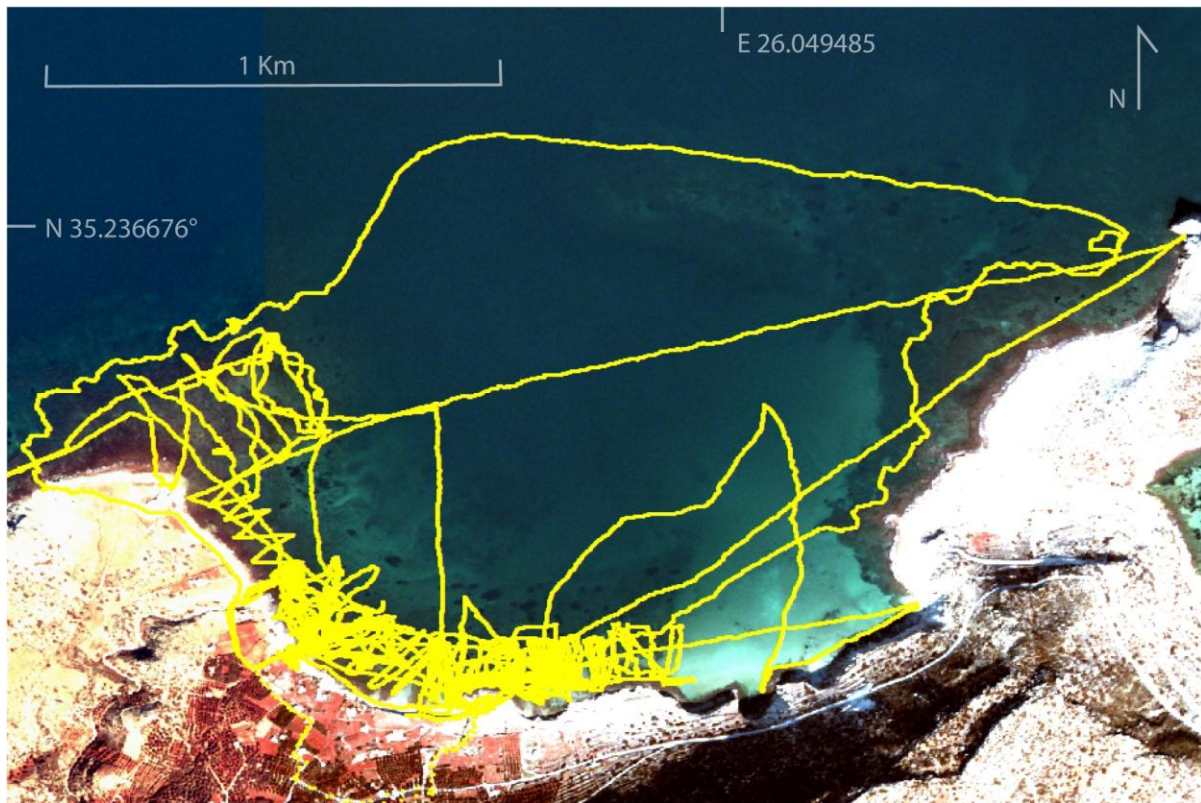


Figure 9. Survey transect pathways

Surveying of all transects was carried out under calm conditions with wave heights of less than 0.3 m to limit depth errors created by wave heave. The US Army Corps of Engineers (US Corp of Engineers 2002) considers conditions with more than a 10 degree pitch or roll to produce an error of more than ± 0.06 m unacceptable for single beam sonar survey work. To produce results within this range of error, our instrument was tested by recording depth measurements over a level surface at 10 degrees of roll and pitch using a level and angle measuring device. A one sample t-test compared the average acoustic depth reading to the measured depth at 1.1 m at a 10 degree roll. At 10 degrees the difference between depth readings ($n=8$) was not significant, $p = 0.82$. A p-value this high provides strong evidence that there is an insignificant difference between measurements. However, in extremely shallow water (<3 m) the beam width of the sonar is small (<1 m), ensonifying a narrow portion of the sea floor. Surface motion has a more dramatic effect on the target recorded and the position recorded for features at these depths. As such, it is imperative to have calm conditions when

surveying in extremely shallow areas. In deeper water, the effect of surface motion has less impact on the depth measurement due to the wider beam width (Figure 10).

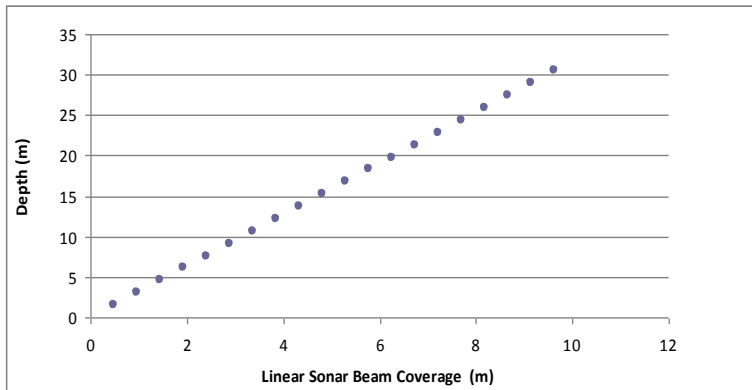


Figure 10. Calculated linear coverage of sonar beam by depth. (See Appendix for formula.).

through hand sampling, accomplished by diving (Desruelles et al. 2009). Without the appropriate infrastructure available for use of SCUBA at Papadiokampos, hand sampling involved free diving to accessible depths to chip samples from the substrate with a hammer. Geologic samples were taken selectively during each transect at locations with superficial changes in the substrate (Figure 11). The position and depth for each sample were recorded with the survey instruments. Each sample was identified and plotted in ArcGIS to determine patterns in substrate composition and stratigraphy in an effort to tie this information to the terrestrial geology.

4.3 SUBSTRATE SAMPLING

Substrate surfaces in the shallow near-shore areas at Papadiokampos are sand, conglomerate, cobbles, sandstone and schist. Samples from these types of substrate are obtained

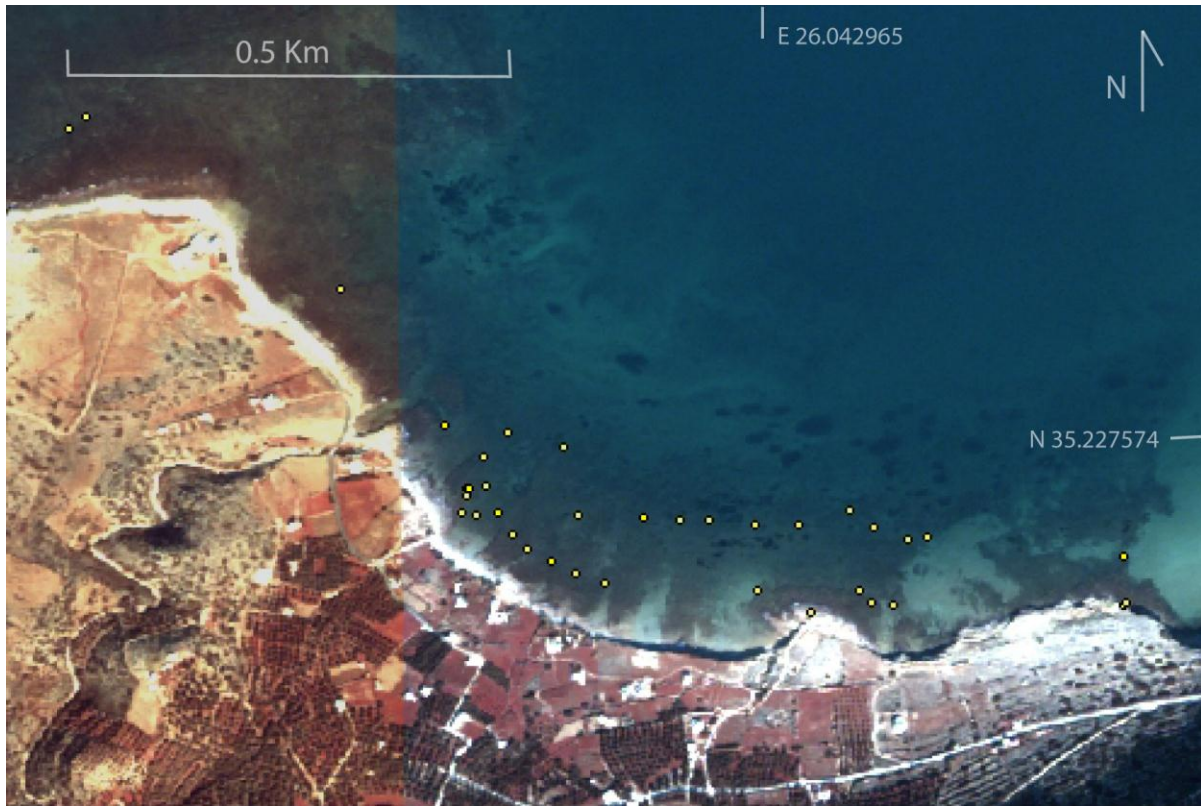


Figure 11. Location of geologic samples indicated by yellow dots.

CHAPTER 5. CONTOUR AND SUBSTRATE MAPPING

Aside from navigation safety, the dynamics of coastal morphology are important to understand as sea level fluctuations and catastrophic events continually change these landscapes. Near-shore bathymetry maps record features of the sea floor that influence wave energy, currents, and sediment erosion or deposition that shape the coastline. Bathymetric maps also record signatures of past coastal landscapes that reveal past responses of shorelines to these changes. These maps are a valuable tool in assessing the potential for coastal change in these dynamic environments.

Data collected during the bathymetric survey at Papadiokampos was used to produce a series of maps that: first, result in a set of contour maps that include bathymetry and topographic data, and second show a substrate classification map with an analysis of relationships between and among substrates.

5.1 CONTOUR MAPS

The following series of contour maps detail the terrestrial and seafloor topography (Figure 12 & 13). Terrestrial topography from the Advanced Spaceborne Thermal Emission and Reflection Radiometer (ASTER) 30 m resolution Global Digital Elevation Model (GDEM) data set was re-projected to match the field-collected bathymetric data set. The bathymetric contour data reveals two shallow submarine peninsulas that protrude from the headlands of the bay. The eastern peninsula is 200 m wide and extends 1.3 km at an average depth of 20 m. The western peninsula is 300 m wide and extends 400 m with an average depth of 5 m.

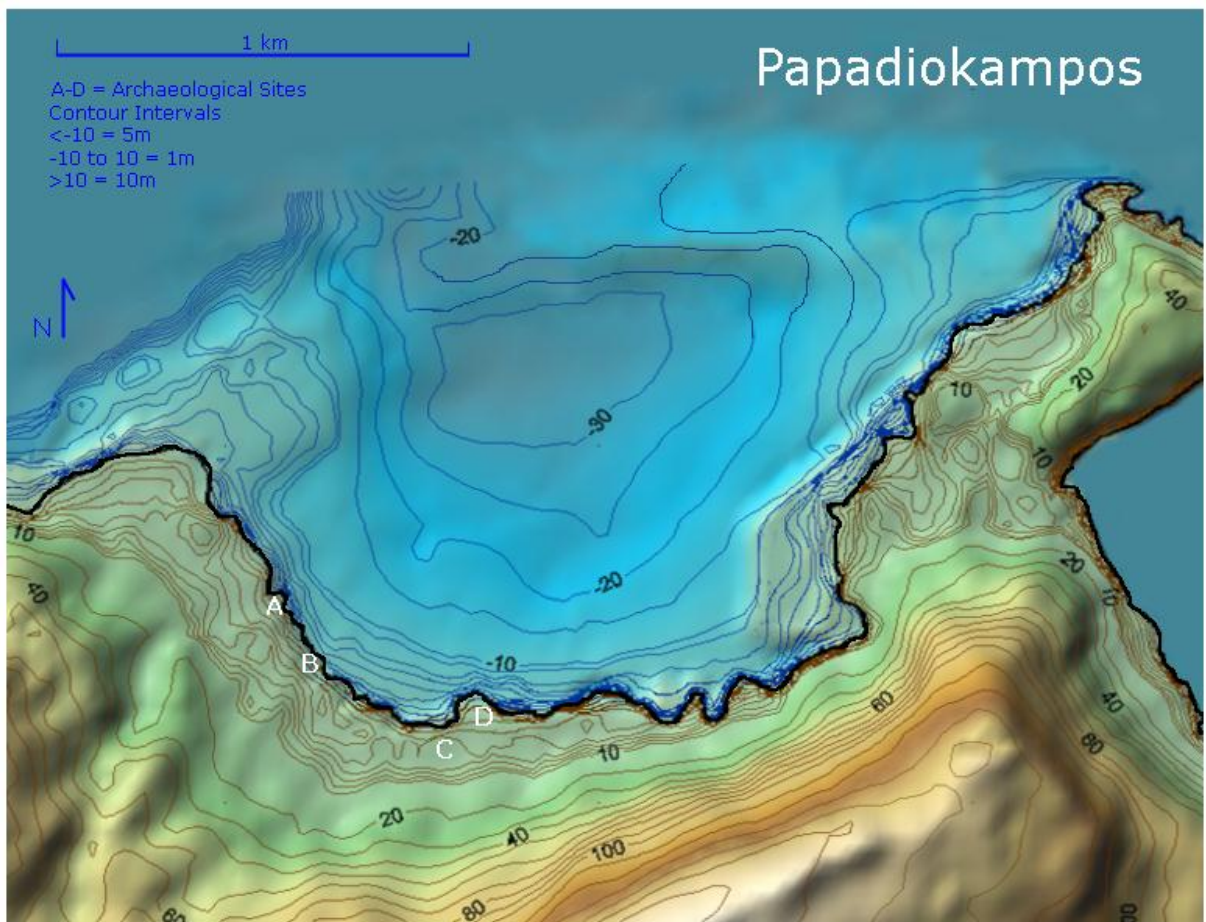


Figure 12. Contour map of Papadiokampos

5.2 SUBSTRATE CLASSIFICATION MAPS

The substrate classification maps (Figures 14 & 15) are supported by the digitization of feature categories and substrate type determined from the underwater camera images, direct observation and geologic sampling. The eastern half of the bay is composed of a large sandy area that grades smoothly

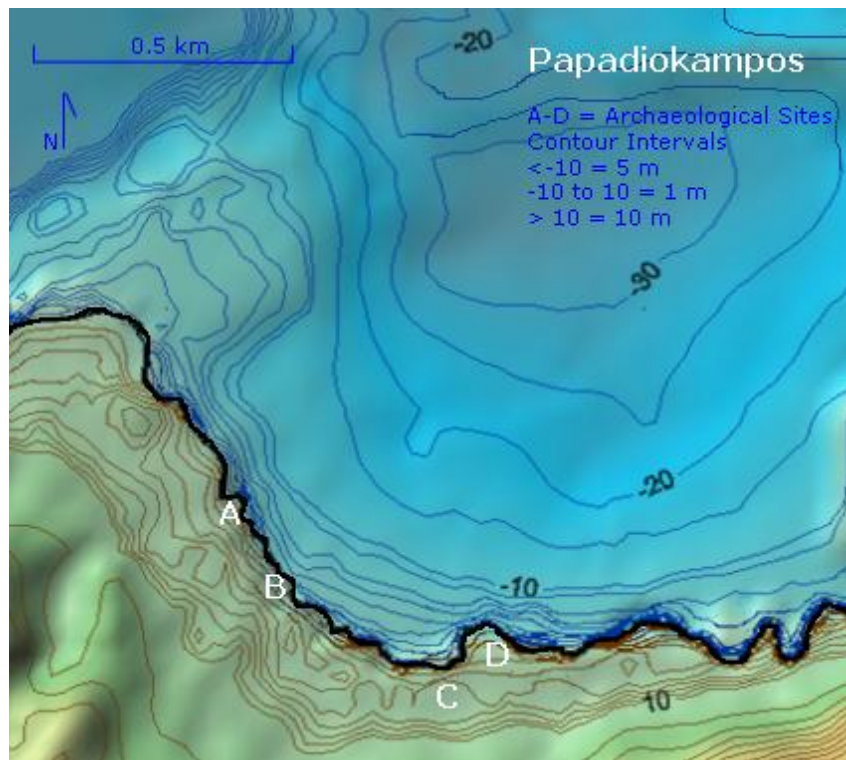


Figure 13. Close up contour map of western side of bay with archaeological sites indicated as A-D.

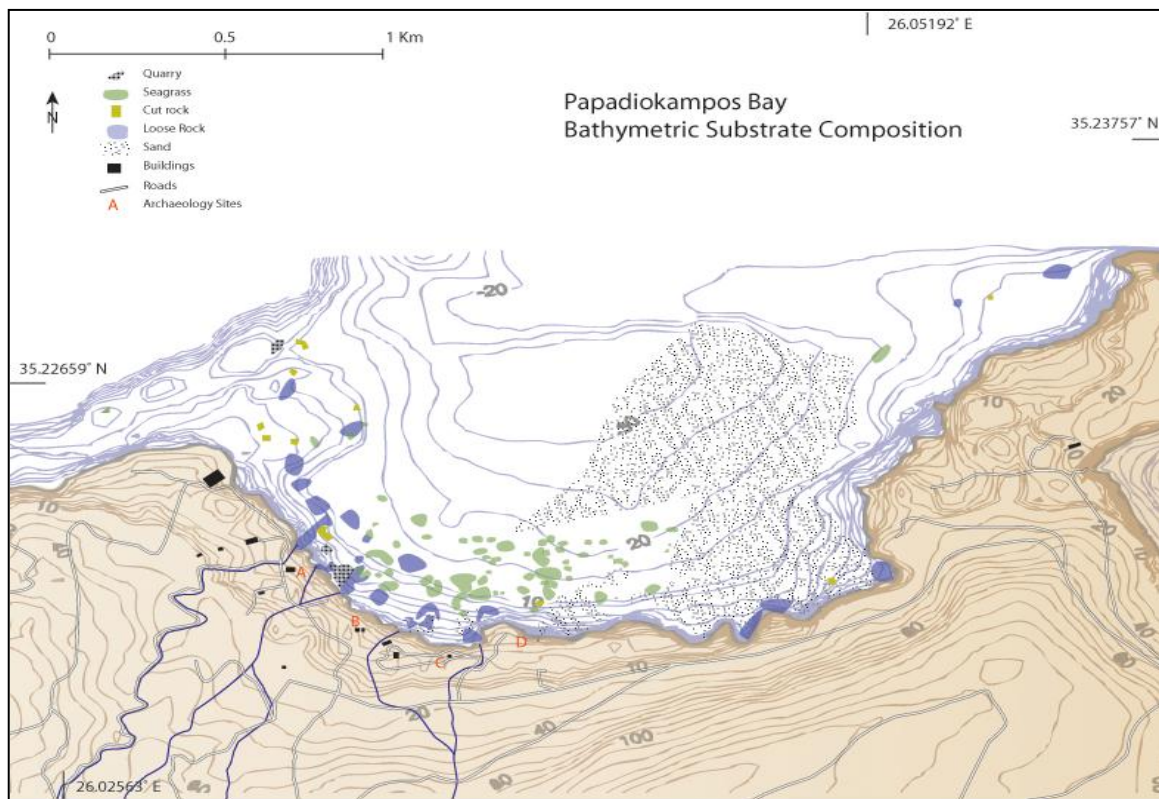


Figure 14. Bathymetric substrate classification map of Papadiokampos Bay. All substrates that are unclassified(white) are solid rock.

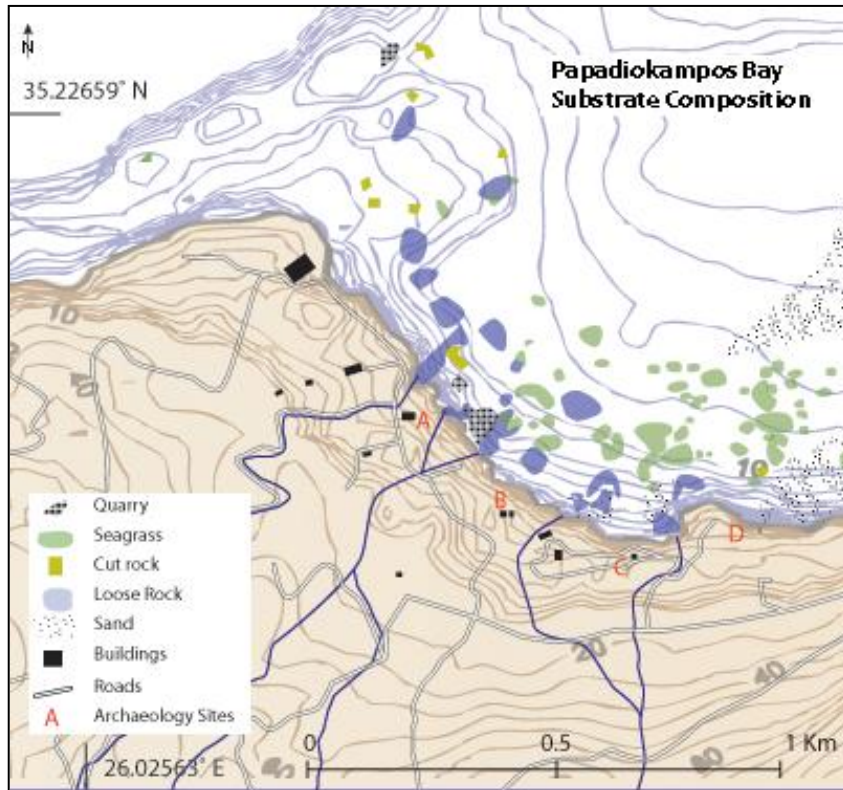


Figure 15. Close up of substrate classification for western side of Papadiokampos Bay.

from rocky vertical cliffs on shore to the deep central mouth of the bay. A 96 m long bench of beachrock is located in ankle deep water in front of the cliffs along the central portion of the shoreline. Seagrass beds are concentrated between the 5 m and 15 m isobaths. Loose rocks are associated with stream outlets along the shoreline. Relict stream beds now underwater align with stream beds on the modern surface or with stream channels that cut through

the cliff face onshore suggesting that these streams were active in the past as well.

A beachrock deposit is concentrated along the foot of the central shoreline cliff face between areas B and C, where two streams enter the bay. The combination of freshwater (as groundwater) and a continuous supply of eroded sedimentary sand from the cliff allowed beachrock to form in this location.

In addition to natural features, human-made rock-cuts were identified in several areas on the western side of the bay (Figure 16). The rock-cut patterns are similar to quarry cuts documented in other ancient settlements on the island (Figure 17). The rock is composed of grey and pink colored schist that splits readily along foliated planes. The three largest rock-cut areas (indicated as quarries on the substrate maps) are located between -2 to -9.6 m depth, covering areas that range from 52.2 m² to 773.4 m². Rectangular and square cuts range from 50 x 30 cm to 3 x 3 m throughout these areas. Long incisions made in the rock that allow shaping and extraction of a block, range from 5cm to 1.5 m deep.

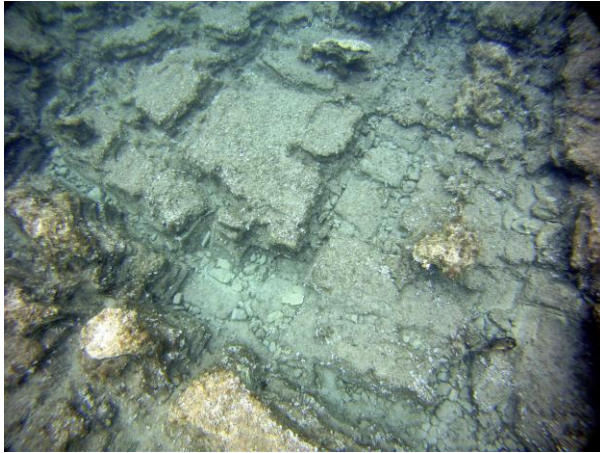


Figure 16. Rock cuts in schist underwater at Papadiokampos with multi-level horizontal planes and variable size and shape blocks similar to ancient quarries on the island.



Figure 17. Subaerial rock cuts in limestone at an ancient quarry in western Crete. This area was uplifted 9 m and would have been just above sea level prior to uplift.

CHAPTER 6. RESULTS AND CONCLUSIONS

This chapter reports on the accuracy of field data collected and the resulting maps. The results of the survey at Papadiokampos will be applied to the research objectives outlined earlier. Concluding statements are made and a summary of the research is given. The implications of this research are discussed and suggestions are made for further research in this area.

6.1 ACCURACY ASSESSMENT OF FIELD DATA COLLECTION AND MAPS

All bathymetric surveys include a range of error. Three types of error exist: blunders, systematic errors and random errors. Blunders are potential errors caused by the surveyor and can be avoided through careful and attentive practices. Systematic errors are the result of a predictable source such as inaccurate calibration of an instrument or tidal fluctuations during a survey and can be corrected once identified. Random errors are not predictable and may be caused by variation in the sea floor between samples or interpolation methods.

Errors can be minimized and calculated to determine the confidence we have in the final map product. The survey instruments and methods used in this study are evaluated by referring to the standards set by three entities: the US Army Corps of Engineers, who are responsible for evaluating the navigability of US waterways; the Federal Geographic Data Committee (FGDC), who developed the National Standard for Spatial Data Accuracy (NSSDA) which includes standards for GPS surveys; and the USGS, who is responsible for the collection, processing and quality control of national Digital Elevation Model (DEM) data for the United States.

6.1.1 Bathymetric (vertical) survey assessment

All depth measurements, regardless of the method used, require a correction for local variations in sea level due to tide changes and atmospheric conditions that produce a discrepancy between measurements of depth taken at different times. This correction is achieved through reference to local tide gauge and weather station centers (Desruelles et al. 2009, Anzidei et al. 2011, Mourtzas 2012a). Corrections in the Mediterranean Sea are slight because the tidal range varies by ± 0.2 m to ± 0.3 m during the duration of surveys and atmospheric pressure changes cause a maximum fluctuation of ± 0.5 m (Desruelles et al. 2009).

Bathymetric surveys are classified into three broad groupings – Contract/Class 1, Design/Class 2 and Reconnaissance/Class 3. Accuracy standards for each survey type are established by the FGDC (Table 1).

Table 1. FGDC accuracy standards for bathymetric surveys (FGDC 1998).

Type of survey	Vertical accuracy (mm)	Horizontal positioning (m)
Class 1	150	6
Class 2	300	12
Class 3	500	100

The vertical accuracy of the sonar instrument used at Papadiokampos is stated by Garmin as ± 23 cm at < 10 m depth, and ± 1 m at > 10 m depth. Vertical accuracy for this survey was calculated by comparing a series of manually measured depths to the sonar recorded depth at a given location. Using the NSSDA the Root Mean Square Error (RMSE) is computed as 0.23 m using the following equation:

$$RMSE_z = \sqrt{\frac{\sum (Z_{data\ i} - Z_{check\ i})^2}{n}}$$

where:

RMSE is the Root Mean Square Error (m)

$Z_{data\ i}$ is the vertical value of the i th data point

$Z_{check\ i}$ is the vertical value of the i th data check point

i is an integer from 1 to n

n is the number of points being checked (36)

From the RMSE figure, the vertical accuracy at the 95 percent confidence level A_z is calculated as 0.45 m using the following equation (assuming a minimum of 30 data check points): $A_z = 1.960 * RMSE_z$ (Greenwalt and Schultz 1968)

The results of this analysis show that the vertical data included in the maps presented here have 0.45 m fundamental vertical accuracy at the 95 percent confidence interval. The vertical accuracy of the maps are therefore stated as ± 0.45 m.

6.1.2 GPS (horizontal) survey assessment

There are many recognized types of GPS surveys including - Autonomous, Static, Fast Static, Post Processed Kinematic, Real Time Kinematic, Continuous Kinematic, Airborne GPS, Networked RTK and Code Based Data Collection. Autonomous, or hand-held GPS surveys give an immediate position without any post processing or signal corrections. A hand-held GPS unit is used to determine an approximate position of a target within 5-10 m. This survey type has the lowest order of accuracy. The positioning accuracy of the system we used would be improved through the use of a dGPS. However, until base stations or virtual reference station networks are established in these remote areas, dGPS is not a viable option. In remote areas, like Papadiokampos, autonomous GPS is often the only option for surveys because of the demanding conditions, unavailability of established control points, or signal correction towers, that do not exist. However, this type of survey is appropriate for reconnaissance or baseline studies such as the one conducted in this study.

To establish a reference point for calculating the error within an Autonomous GPS survey a long-term averaging of position approach was used. A GPS receiver was set up to store positions at a regular interval over a fixed position for as long as possible. Longer time periods of position collection result in better average positioning. A 24-hour observation period is preferable to obtain point position accuracy to the meter-level. At Papadiokampos, a reference point was established by setting a GPS receiver to collect position fixes continuously over a fixed location for a period of 2 hours. The long-term average position for this point was established as N 35 13.29 and E 26 2.37.

The National Geodetic Survey (NGS) has established accuracy standards for GPS surveys (Table 2). An autonomous survey follows the accuracy standards for a third order survey.

Table 2. NGS Accuracy standards for GPS surveys (NGS 1989).

Classification	Minimum Geometric Accuracy Standard*
AA - Order	0.3 cm ± 1:100,000,000
A - Order	0.5 cm ± 1:10,000,000
B - Order	0.8 cm ± 1:1,000,000
First - Order	1.0 cm ± 1:100,000
Second - Order, Class I	2.0 cm ± 1:50,000
Second - Order, Class II	3.0 cm ± 1:20,000
Third - Order	5.0 cm ± 1:10,000

*At the 95% Confidence Interval

The horizontal accuracy of the GPS unit used in this survey is stated as <5 m (with EGNOS enabled). The horizontal accuracy in this survey calculated by comparing an established control point position to a single GPS position recorded during the survey twice each day. The RMSE is computed as 0.32 m using the following FGDC NSSDA equation:

$$RMSE_h = \sqrt{\sum((X_{data\ i} - X_{check\ i})^2 + (Y_{data\ i} - Y_{check\ i})^2)/n}$$

where:

RMSE_h is the Root Mean Square Error (m)

X_{data i} is the horizontal x-axis coordinate of the ith data point

X_{check i} is the horizontal x-axis coordinate of the ith data check point

Y_{data i} is the horizontal y-axis coordinate of the ith data point

Y_{check i} is the horizontal y-axis coordinate of the ith data check point

n is the number of check points tested (36)

i is an integer ranging from 1 to n

From the RMSE figure, the horizontal accuracy at the 95 percent confidence level A_h is calculated as 0.55 m using the following equation:

$$\begin{aligned} A_h &= 2.4477 * RMSE_x = 2.4477 * RMSE_y \\ &= 2.4477 * RMSE_h / 1.4142 \end{aligned}$$

$$A_h = 1.7308 * RMSE_h \quad (\text{Greenwalt and Schultz 1968})$$

The horizontal error calculated for the bathymetric survey is considerably lower than the error range of the instrument. Given the vertical and horizontal accuracy assessment for this bathymetric survey, the results should be considered as a Reconnaissance/Class 3 type survey.

The number of data points collected over a given area also affects the accuracy of bathymetric surveys. The US Army Corps of Engineers recognizes that 2-3 points/100 m² is the lowest acceptable data density for bathymetric surveys. The total area surveyed at Papadiokampos is 1,983,815 m² with 41,974 points collected. This equates to a total coverage of 2 points/100 m². However, survey efforts were concentrated in areas adjacent to the excavation sites and had a higher density of data points. 21,827 points were collected in an area of 133,567 m², which equates to a coverage of 16 points/100 m² within the survey focus area.

6.1.3 Digital Elevation Model accuracy assessment

DEMs are an array of regularly spaced elevation data. The space between data points is determined through interpolation. The accuracy of the DEM data is analyzed by comparing the interpolated elevations to a corresponding map location elevation or verification point and calculating the RMSE. The RMSE formula is written as:

$$\text{RMSE} = \sqrt{\frac{\sum (f(x_i) - y_i)^2}{n}}$$

where:

x_i is the interpolated elevation point, and

y_i is the verification point.

The smaller the RMSE the closer the interpolation model resembles the verified terrain. USGS standards require 28 verification points to calculate the RMSE for DEM's, 8 of which need to be edge points. USGS standards of accuracy established for DEMs are listed in Table 3. Kriging (Matheron 1963) was used to interpolate data values for areas between surveyed points. To evaluate the error in the DEM created in this study, the uncertainty associated with the Kriging interpolation method is examined through a comparison of modeled elevations and corresponding verification points. Verification points are recommended by the USGS in order of preference as field control points, aerotriangulated test points, spot elevations, or points on contours from existing source maps with appropriate contour intervals. Because established

verification points were not available for the underwater area, verification points in this study were established through spot depth measurements using a weighted measuring tape. The RMSE calculated for the DEM of Papadiokampos is 0.98 m. With a contour interval of 10 m, a level 3 DEM is achieved.

Table 3. USGS accuracy standards for DEMs (USGS 1997).

Classification	Accuracy Standard
Level 1	RMSE of 7-15 m
Level 2	RMSE max of half a contour interval with no errors more than one contour interval.
Level 3	RMSE max of one third a contour interval with no errors more than two thirds of a contour interval.

The accuracy of the DEM model was quantified using a linear regression and the 95 percent Confidence Interval of the error. From each linear regression, the R^2 value was determined. The R^2 value is high (close to 1), confirming that the interpolation methods worked well with this data set. A high value and a narrow range of the R^2 value indicates that all methods were essentially equivalent for this data set (Figure 18).

The next step in describing the accuracy of the modeled surface is to determine the elevation Confidence Interval. The 95 percent Confidence Interval was calculated using the following equation (McClave and Sincich 1997):

$$\bar{x} \pm z_{a/2} [s/\sqrt{n}]$$

where:

\bar{x} is the mean (7.3 m),

$z_{a/2}$ is the z-value at a specified

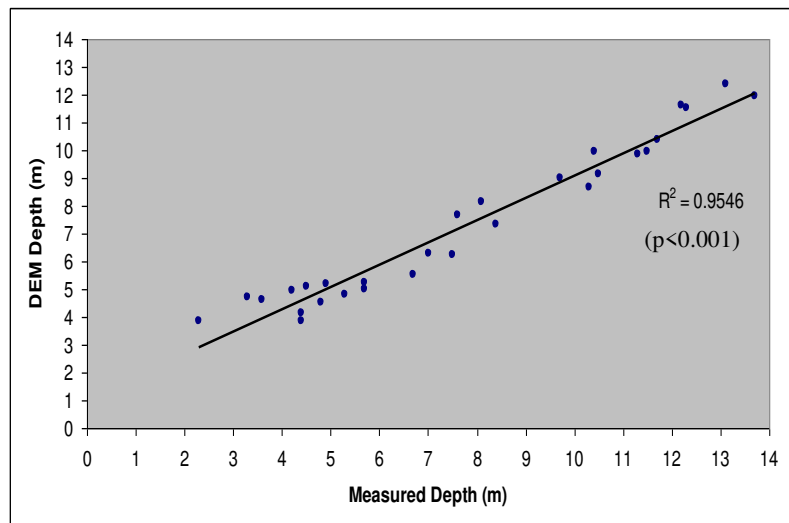


Figure 18. Linear regression analysis of DEM for 30 points across Papadiokampos Bay survey area.

confidence level (1.96 at 95%),

s is the standard deviation (2.8 m),

and n is the population size (number of verification points = 30)

The estimate 95% confidence, the true depth lies within ± 1 m on the DEM. This is within error range of the sonar instrument in depths greater than 10 m, which encompasses most of the area surveyed.

6.2 RESEARCH OBJECTIVES

Research objective #1 – Location of the Bronze Age Shoreline

The archaeological record indicates that the Bronze Age inhabitants of Papadiokampos permanently abandoned the area during the LMII period (1400-1450 BC) (Sofianou and Brogan 2009). This area was never re-occupied and remains nearly deserted today. During the course of this bathymetric survey, human-made rock cuts were identified on the seafloor at depths between -2 to -9 m. To be functional, these rock-cut areas would have to be at least 0.6 m above mean sea level (Scicchitano et al. 2008) during the time of use. Paving stones within the archaeological excavation of Bronze Age structures on shore at Papadiokampos as well as further east on the coast at Palaikastro (MacGillivray et al. 1984) are identical to the rock type from these cuts (Figure 19). This indicates that this rock type was certainly used during the Bronze Age and that it was used on site and likely transported by boat to other coastal



Figure 19. Schist paving stones within the excavation area A at Papadiokampos with stone types identical to those of the cut stone found underwater nearby.

settlements. This implies that the last time this rock was cut was during the Bronze Age occupation of this area when sea level was at least -9.6 m lower than today.

Near the rock-cut areas, wave-cut notches are eroded in the seafloor substrate at an average depth of -10 m along the western side of the bay. These notches represent a sea level 10.3 m lower than today and provide the best indicator for shoreline position during the Bronze Age. This relict

shoreline indicates a sea level that is significantly lower than the modeled estimates for this time period of -3.45 m (Lambeck 1995). This discrepancy suggests that vertical tectonic movement has been a significant factor in shaping the shoreline over time. The implications of earthquake activity are varied but known to cause the destruction of harbors and coastal dwellings in antiquity (Guidoboni and Comastri 1997). While it is unknown why the Bronze Age inhabitants left this area, the submerged landscape features suggest that an abrupt change in the coastal morphology occurred, likely caused by a large vertical tectonic shift.

A sea level -10.3 m lower than today would reveal a very different coastal morphology. The western peninsula would have been subaerial and a shallow shoal would have extend from the eastern headland providing a barrier of protection against storm surge and wave energy. This is important to consider because some coastal morphologies such as peninsulas and small off-shore islands were preferred areas of settlement during the Bronze Age (Shaw 1990).

A reconstruction of the Bronze Age shoreline, based on the submerged geomorphic evidence gathered during this study (Figure 20) illustrates a landscape that once resembled an area of settlement preference for early inhabitants (Shaw 1990). The bay would have been naturally protected and the rock cut areas would be located in close proximity to shore allowing for transport by sea. Submerged rock mooring bollards suggest the presence of a harbor. The presence of a harbor is also supported by established indicators of ancient harbors (Goiran and Morhange 2003); a natural low energy environment and a depth capable of accommodating vessel draught - a minimum 1 m depth (Marriner and Morhange 2007). Large swaths of loose rock adjacent to rock-cutting areas also suggest a harbor environment where vessels could be pulled ashore (Wachsmann 1999).

When relative sea level rose, submersion of this peninsula allowed more wave energy to enter the bay, destroying the protection this land mass once offered. All of the rock cuts located on the peninsula were submerged with the 10.3 m shoreline. Losing valuable coastal resources and a protected harbor, possibly in an abrupt seismic event must have had a significant impact on the population.

Research objective #2 - Spatial sequence of coastal change at Papadiokampos

During the course of the bathymetric survey, wave cut notches were identified at three depths -5.7 m, -7.7 m and -10.3 m. Compared to today's shoreline, 727,515 m² of land has been submerged since the -10.3 m shoreline was active, with a transgression ranging from 28 to 178 m inland. The most significant transgression would have occurred over the western peninsula. A second series of wave-cut notches is located offshore at -5.7 m depth. By the time sea level rose from -10.3 m to -5.7 m an area of 102,549 m² would have been submerged including most of the peninsula and remaining rock cut areas. Today the western peninsula is completely submerged as well as all of the rock cut areas. The submerged peninsula now buffers currents from the open sea but surface waves enter the bay unobstructed.

The wave-cut notches are eroded into non-conglomerate rock types. The erosion pattern underwater resembles wave-cut notches along the modern shoreline. Collapsed undercut visors located underwater are associated with conglomerate rock types. These features are plentiful outside the sandy substrate areas of the bay and resemble collapsed visors along the modern shoreline (Figure 7). The similarity in structure and morphology of these features provides supporting evidence that these are past shoreline features. Unfortunately, the geologic samples collected from these features did not contain any datable material that would allow assignment of the rate of transgression.

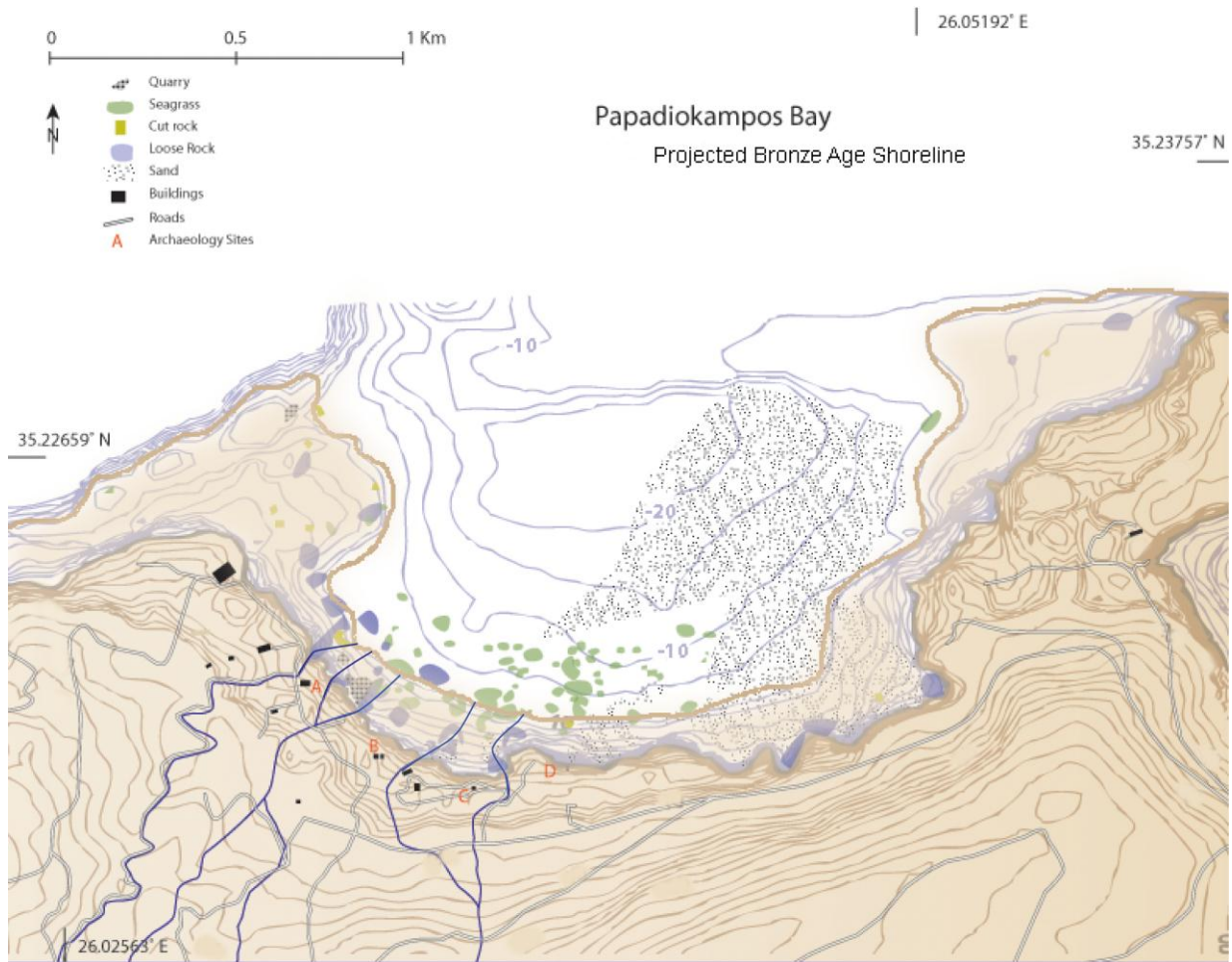


Figure 20. Projected Bronze Age shoreline with modern substrate features indicated.

Research objective #3 –Temporal pace of shoreline change since the Bronze Age

The seafloor of Papadiokampos Bay is comprised of five substrate types: solid rock (sandstone, schist and marble), sand, loose rock & boulders, beachrock and conglomerate rock. The biota is extremely limited and inspection of the samples collected did not yield any datable ^{14}C material. With future funding resources, the beachrock formations near shore could provide temporal information from radiocarbon dating of the diagenetic cement that forms between sand grains in the intertidal zone during periods of sea level stability (Desruelles et al. 2009). In other studies, beachrock in western Liguria, Italy revealed a sea level pause at 3,330 \pm 95 years BP at +0.5 m to -4.0 m (Gewelt and Fierro 1983), and in the Cyclades islands north of Crete, beachrock dating indicates a sea level pause at 4,000 years BP at 3.6 m (Desruelles et al. 2009).

This suggests that the 5.7 m shoreline identified at Papadiokampos could be older than 4,000 years.

The only archaeological remains identified on the seafloor were rock cuts in the substrate. These provide a relative date for the time period cuts were made which would have been during the occupation of this area prior to 1450 BC. The deepest rock cut edge is at -9m depth, which indicates that the submerged wave cut notches identified nearby likely formed during the Bronze Age. This would indicate that the shoreline has submerged 10.3 m and moved a minimum of 28 m inland over the past 3463 years.

The preservation of wave cut notches at -7.7 m and -5.7 m indicate pauses in sea level followed by abrupt changes in sea level consistent with vertical tectonic movement. This indicates that the coastal morphology at Papadiokampos changed drastically at least twice since the Bronze Age.

6.3 RESEARCH SUMMARY

The bathymetric survey conducted at Papadiokampos reveals a lost landscape partially preserved through submersion. Two abrupt changes in the vertical position of the shoreline (indicated by preservation of shoreline features on the seafloor) drastically changed the morphology of the coastal landscape since the Bronze Age, submerging a protective peninsula and an important coastal resource – a rock quarry. The slower processes of sea level rise and isostatic adjustment are eroding the shoreline slowly today, obliterating all but the most resistant rock types such as marble and schist. The modern shoreline is largely composed of sedimentary conglomerate and sandstone, which is responding to these erosional processes leaving virtually no trace of shoreline positions of the most recent past.

6.4 IMPLICATIONS OF RESEARCH AND FUTURE STUDY

Adaptation is being encouraged as sea level across the world continues to change. If the evidence at Papadiokampos is any indication of the vulnerability of large coastal populations under the influence of tectonic movement and sea level rise, efforts need to be concentrated in these areas to protect people and resources. Adaptation to sea level change efforts include

planned retreat (Niven and Bardsley 2013), sewer desiltation (Dasgupta et al. 2013), raising awareness of risk (Jin and Francisco 2013), beach nourishment (Mycoo and Chadwick 2012), livelihood changes (Morand et al. 2012), diversified and decentralized critical infrastructure (Shahid 2012), flood protection and enhanced water management (Bormann et al. 2012). Yet, these adaptations may not be enough as this work indicates where rapid shoreline changes occurred, with three abrupt shifts during a span of 3600 years. These changes should be expected and designed for where the double risk of sea level rise and high seismic activity put coastal land area and resources at risk. A shrinking space with a growing population is a squeeze that will not continue to be supported by these landscapes.

Dealing with earthquakes is a more difficult matter. Without any way to predict when an earthquake will strike or how powerful it will be (Kagan and Jackson 2000), adaptation is not plausible. Preparation and response planning are needed to help alleviate damage from tectonic activity. Understanding the way an area has responded to tectonic movement in the past will strengthen our capability to plan appropriately and deal more effectively with earthquake activity on a local scale.

Understanding local variations in coastal change due to sea level change as well as tectonic activity is critical to protect life and livelihoods. Loss of land, coastal resources and infrastructure is especially a concern in areas that are over-populated and impoverished. While sea level change and tectonic movement vary greatly across the globe and across regions so must our approach to solutions. The study of past coastal morphology in these areas can improve our ability not only to adapt and protect, but also enhance our capability of identifying highly vulnerable areas and being better prepared to face these changes.

APPENDIX

The results of testing which investigate the physics of the acoustic technology (SONAR) used to record water depth at the research site in Crete, Greece are presented here, followed by a list of specifications for each instrument used in this study.

Test 1: Sound velocities for Mediterranean Sea temperature, turbidity and salinity values during the research period.

Sound velocities are calculated with the international standard algorithm, also known as the UNESCO algorithm, by Chen and Millero (1977). The equation for sound velocity is:

$$c(S,T,P) = Cw(T,P) + A(T,P)S + B(T,P)S^{3/2} + D(T,P)S^2$$

$$Cw(T,P) = (C_{00} + C_{01}T + C_{02}T^2 + C_{03}T^3 + C_{04}T^4 + C_{05}T^5) + \\ (C_{10} + C_{11}T + C_{12}T^2 + C_{13}T^3 + C_{14}T^4)P + \\ (C_{20} + C_{21}T + C_{22}T^2 + C_{23}T^3 + C_{24}T^4)P^2 + \\ (C_{30} + C_{31}T + C_{32}T^2)P^3$$

$$A(T,P) = (A_{00} + A_{01}T + A_{02}T^2 + A_{03}T^3 + A_{04}T^4) + \\ (A_{10} + A_{11}T + A_{12}T^2 + A_{13}T^3 + A_{14}T^4)P + \\ (A_{20} + A_{21}T + A_{22}T^2 + A_{23}T^3)P^2 + \\ (A_{30} + A_{31}T + A_{32}T^2)P^3$$

$$B(T,P) = B^{00} + B_{01}T + (B_{10} + B_{11}T)P$$

$$D(T,P) = D_{00} + D_{10}P$$

Where T = temperature in degrees Celsius
S = salinity in Practical Salinity Units (‰)
P = pressure in kPa (100 kPa = 1 bar)
A,B,C,D = Coefficients (Table 4)

Range of validity: temperature 0 to 40 °C
salinity 0 to 40‰
pressure 0 to 100,000 kPa
(Wong and Zhu 1995)

Table 4. Coefficients for sound velocity UNESCO equation (Chen and Millero 1977).

Coefficients	Numerical values	Coefficients	Numerical values
C ₀₀	1402.388	A ₀₂	7.166E-5
C ₀₁	5.03830	A ₀₃	2.008E-6
C ₀₂	-5.81090E-2	A ₀₄	-3.21E-8
C ₀₃	3.3432E-4	A ₁₀	9.4742E-5
C ₀₄	-1.47797E-6	A ₁₁	-1.2583E-5
C ₀₅	3.1419E-9	A ₁₂	-6.4928E-8
C ₁₀	0.153563	A ₁₃	1.0515E-8
C ₁₁	6.8999E-4	A ₁₄	-2.0142E-10
C ₁₂	-8.1829E-6	A ₂₀	-3.9064E-7
C ₁₃	1.3632E-7	A ₂₁	9.1061E-9
C ₁₄	-6.1260E-10	A ₂₂	-1.6009E-10
C ₂₀	3.1260E-5	A ₂₃	7.994E-12
C ₂₁	-1.7111E-6	A ₃₀	1.100E-10
C ₂₂	2.5986E-8	A ₃₁	6.651E-12
C ₂₃	-2.5353E-10	A ₃₂	-3.391E-13
C ₂₄	1.0415E-12	B ₀₀	-1.922E-2
C ₃₀	-9.7729E-9	B ₀₁	-4.42E-5
C ₃₁	3.8513E-10	B ₁₀	7.3637E-5
C ₃₂	-2.3654E-12	B ₁₁	1.7950E-7
A ₀₀	1.389	D ₀₀	1.727E-3
A ₀₁	-1.262E-2	D ₁₀	-7.9836E-6

In seawater, temperature, turbidity, pressure and salinity affect the sound velocity. Sound travels quickest through warm, clear, dense (high salinity, deep) water, especially at low frequencies. In this study, with shallow, clear, sea water, variability in temperature will affect the sound velocity more readily than salinity, depth or turbidity.

These rates of change are as follows:

A 1°C change in temperature = 3 m/s change in sound velocity

A 1 ‰ change in salinity = 1.3 m/s change in sound velocity

At 100 m depth the sound velocity changes by 1.7 m/s (Hall 2000)

Water samples were taken at 3 depths (10 m, 5 m and surface) at Papadiokampos during the summer 2011 survey. Measurements of salinity, temperature and turbidity for each sample allow calculation of the sound velocity for conditions specific to this site. Measurements for water parameters at the study site are as follows:

Salinity and Temperature were stable to 10 meter depths:

Salinity (S) = 37 ‰

Temperature (T) = 23.3°C

Turbidity was variable at all depths measured:

10 m turbidity = 0.18 NTU

5 m turbidity = 0.24 NTU

Surface turbidity = 0.06 NTU

Turbidity measurements are so minute that the effect on sound velocity in this case is inconsequential.

Solution: The sound velocity calculated for water parameters at Papadiokampos from 0 to 10 meters depth is 1492.09 m s⁻¹.

Test 2: Acoustic wavelength for the frequency used.

The equation for wavelength is: $\lambda = 1000 \times \text{square root of } 10/(f\sigma)$

Where λ is the wavelength in m

f is the frequency in Hz

σ is the conductivity in Siemen m⁻¹

(mean seawater conductivity is 3.2 S m⁻¹)

(Manoj et al. 2006)

Solution: The wavelength calculated for the frequency of our instrument (160 kHz) is 6.2 mm. Targets that are larger than one wavelength (6.2 mm) will produce an acoustic return.

Test 3: Shallow water limit of depth readings for the frequency used.

Garmin states the shallow water limit of the sonar we are using is 0.9 m. However, readings of 0.3 m were recorded in initial surveys. To determine the accuracy and limit of the depth recording for this specific instrument, transects were conducted on January 17, 2012 over a smooth, sand covered, gentle slope in calm water from 1.5 m depth to 0 m depth (Figure 21)*. The transect was repeated in reverse to confirm the limits of shallow water recordings (Figure 22).

*All acoustic depths have been adjusted by + 0.2 m for the draft of the transducer.

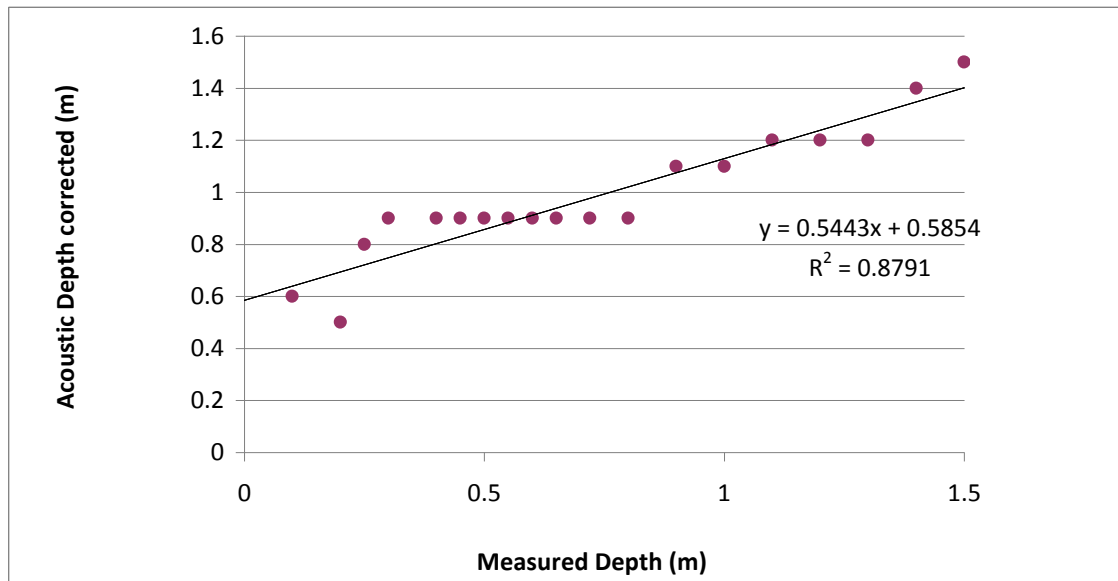


Figure 21. Shallow water limit test transect from 1.5 m to 0 m.

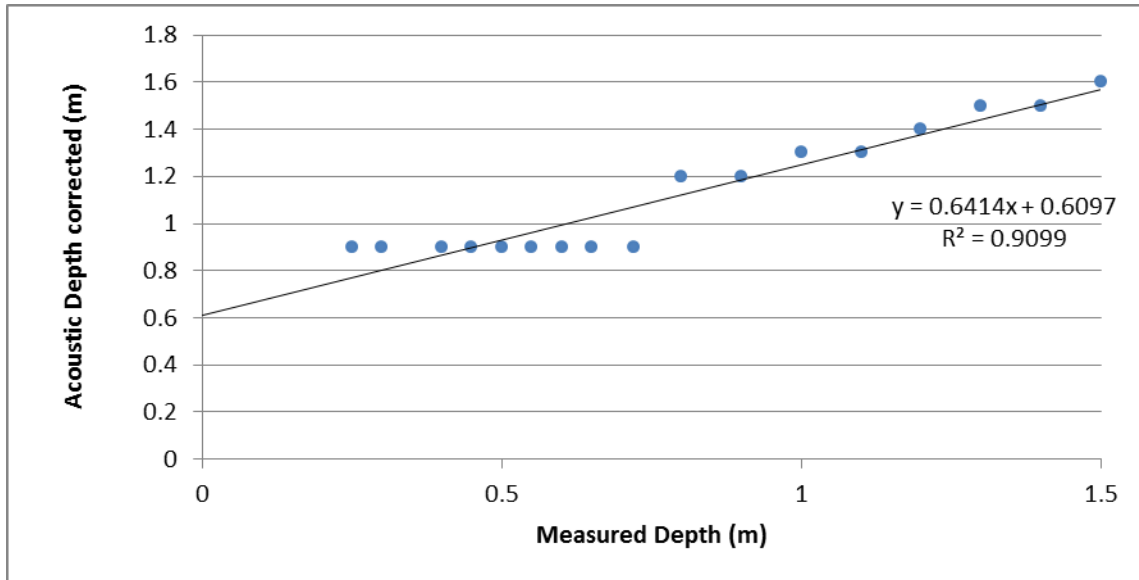


Figure 22. Shallow water limit test transect from 0 to 1.5 m.

The acoustic depth recordings have a mean value of 0.9 ± 0.44 m with a CV of 49.2%. The measured depth recordings have a mean value of 0.75 ± 0.87 m with a CV of 115%. Testing suggests a greater capacity to detect shallow depths when approaching from a deeper area. When beginning from a shallow depth (<0.9 m), recordings do not register until the 0.9 m depth is reached.

Solution: Testing confirms the depth of 0.9 m as the shallowest reliable recording depth for this instrument.

Test 4: Variability of depth reading over a single position in shallow water.

The sonar transducer was held at measured depths of 1.2 m and 0.9 m for 1-minute each to record a static shallow water depth (Table 5).

Table 5. One minute depth reading at 1.2 m and 0.9 m.
 (Acoustic Depth corrected = ADc, Measured Depth = MD).

ADc (m)	MD (m)
1.3	1.2
1.4	1.2
1.3	1.2
1.4	1.2
1.5	1.2
1.3	1.2
1.3	1.2
1.4	1.2
1.3	1.2
1.3	1.2
0.9	0.9
0.9	0.9
0.9	0.9
1.1	0.9
0.9	0.9
0.9	0.9
0.9	0.9
1.1	0.9
0.9	0.9
0.9	0.9

The recorded acoustic depth is deeper than the measured depth of 1.2 m on average. The average acoustic depth measurement is 1.35 ± 0.07 m with a CV of 5.2%. A one sample analysis reveals that there is a significant difference between acoustic and measured depth averages at 1.2 m, $p < .0001$ (Table 6).

Table 6. One sample analysis for 1.2 m depth.

Acoustic Depth	
Mean	1.350
Std. Dev.	.071
Count	10
Minimum	1.300
Maximum	1.500
Coef. Var.	.052
Range	.200
Mode	1.300

One Sample Analysis						
Hypothesized Mean = 1.2						
	Mean	DF	t-Value	P-Value	95% Lower	95% Upper
Acoustic Depth	1.350	9	6.708	<.0001	1.299	1.401

The recorded acoustic depth is deeper than the measured depth of 0.9 m on average. The average acoustic depth measurement is 0.94 ± 0.08 m with a CV of 9%. A one sample analysis reveals that there is not a significant difference between acoustic and measured depth averages at 0.9 m, $p = 0.1679$ (Table 7).

Table 7. One sample analysis for 0.9 m depth.

Acoustic Depth	
Mean	.940
Std. Dev.	.084
Count	10
Minimum	.900
Maximum	1.100
Coef. Var.	.090
Range	.200
Median	.900

One Sample Analysis						
Hypothesized Mean = .9						
	Mean	DF	t-Value	P-Value	95% Lower	95% Upper
Acoustic Depth	.940	9	1.500	.1679	.880	1.000

Solution: The acoustic measurements are all consistently deeper than the measured depth, and the depth accuracy for this instrument declines in deeper water. This testing suggests that the depth accuracy declines much quicker with depth than the stated rate of ± 10 cm at 0-10 m. Additional testing in a larger range of depths up to 10 m would determine if this is true. Regardless, transects should be conducted in 0.9 - 10 m water depth for best accuracy.

Test 5: Acoustic reflectivity differences over different seafloor substrates.

Hard, dense surfaces produce a quicker return because the sound is unimpeded during reflection, like the echo of your voice in an empty room. Soft, permeable surfaces such as deep silt or sea grass impede the acoustic reflection (Urlick 1975). Impedance is calculated using the equation:

$$z = cr$$

Where z = acoustic impedance measured in Rayl (1 Rayl = 1 kg/m²/s)

c = sound speed m s⁻¹

r = density kg m⁻²

A Rayl greater than 0 means that most of the wave will be reflected without any change, (example: steel)

A Rayl equal to 0 means that there is no reflection, (example: sea water)

A Rayl less than 0 means most of the wave is reflected with 180 degree of change (example: air).

Table 8 lists Impedance measurements for a range of materials.

Table 8. Impedance of materials (Lanbo 2006).

Material	Impedance (z)	Rayl (R)
Air	415	-1
Fresh water	1.48 x 10 ⁶	0.04
Salt water	1.54 x 10 ⁶	0
Wet fish flesh	1.6 x 10 ⁶	0.02
Rubber	1.81 x 10 ⁶	0.08
Wet fish bone	2.5 x 10 ⁶	0.24
Clay	7.7 x 10 ⁶	0.67
Sandstone	7.7 x 10 ⁶	0.66
Concrete	8.0 x 10 ⁶	0.68
Granite	1.6 x 10 ⁷	0.82

These values indicate that the materials we are most likely to encounter for an ocean substrate, sandstone and granite, will have the least acoustic impedance, and therefore the quickest returns. This also suggests that some acoustic returns for fish should be expected. However, fish populations are sparse in the Mediterranean and were not encountered during

surveys in this study. Testing the sonar on different substrates in the same water depth determines if the recorded depth changes with substrate composition. Testing in calm water on a level sandy bottom, then on a level cement bottom at the same depth will determine the effect of different substrates on the depth recording of the instrument. During testing, the transducer was held in one position for one minute over each substrate (Table 9).

Table 9. Cement and sand substrate measurement comparison at 1.1 m depth.

ADc	MD	Substrate type
1.1	1.1	cement
1.1	1.1	cement
1.2	1.1	cement
1.2	1.1	cement
1.2	1.1	cement
1.1	1.1	cement
1.2	1.1	cement
1.1	1.1	cement
1.2	1.1	cement
0.9	1.1	cement
1.1	1.1	sand
0.9	1.1	sand
1.1	1.1	sand
1.1	1.1	sand
1.1	1.1	sand
0.9	1.1	sand
0.9	1.1	sand
0.9	1.1	sand
1.1	1.1	sand
0.9	1.1	sand

The acoustic depth measurement over a cement substrate at 1.1 m depth produces an average reading of 1.13 ± 0.1 m with a CV of 8.4%. A one-sample analysis comparing the average acoustic measurement to the measured depth of 1.1 m over a cement substrate reveals that there is no significant differences in these measurements for cement, $p = 0.34$.

At the same depth, the acoustic measurement over a sandy substrate records an average reading of 1.0 ± 0.1 m with a CV of 10.5 %. In this case there is a significant difference between measured and acoustic depth for sand substrate, $p = 0.02$. However, the hypothesized mean is only 2.5 cm outside the upper 95% limit. This means there is not a practical difference in the measurement for sand substrate.

A paired t-test is used to compare the two substrates to determine if there is a difference between measurements over sand or cement. The results of this test reveal that there is a statistically significant difference, $p = 0.0019$ (Table 10).

Table 10. One sample analysis and Paired means comparison tests for cement and sand substrate depth measurements.

	Cement Acoustic Depth	Sand Acoustic Depth
Mean	1.130	1.000
Std. Dev.	.095	.105
Count	10	10
Minimum	.900	.900
Maximum	1.200	1.100
# Missing	0	0
Coef. Var.	.084	.105
Range	.300	.200
Median	1.150	1.000

One Sample Analysis

Hypothesized Mean = 1.1

	Mean	DF	t-Value	P-Value	95% Lower	95% Upper
Cement Acoustic Depth	1.130	9	1.000	.3434	1.062	1.198
Sand Acoustic Depth	1.000	9	-3.000	.0150	.925	1.075

Paired Means Comparison

Hypothesized Difference = 0

	Mean Diff.	DF	t-Value	P-Value	95% Lower	95% Upper
Cement Acoustic Depth, Sand Acoustic130	9	4.333	.0019	.062	.198

Solution: Acoustic measurements over a sandy substrate are significantly different from the measured depth. Considering the stated depth error of ± 10 cm in this depth range, the measured depth is just 2.5 cm outside the upper 95% limit of 1.075 m for the acoustic measurements and is not a practical difference in this application.

Test 6: Effect of seafloor rugosity on returned signal strength and acoustic trace.

The acoustic signal produced by the transducer is directional. For example, with a transducer mounted on a floating platform facing the sea floor, the signal produced from the center of the transducer propagates vertically within a 17.5 degree angle. The acoustic signal reflects off the first object encountered - the shallowest sea floor feature. The reflected signal returns propagating in all directions, the first return is the one recorded. Therefore, regardless of the slope or irregularity of the sea floor, the first object encountered within the ensonified area will be the recorded depth for that signal. Care should be taken in high relief areas where a shallow feature such as a bench-top located at the edge of the beam may return a signal before a deeper feature such as the foot of the bench, which is directly below the transducer. This scenario produces an offset in the recorded position for the shallow feature.

Solution: Regardless of the irregularity of the sea floor substrate, the shallowest feature within the ensonified area will produce the first acoustic return and be recorded as the depth.

Test 7: Acoustic coverage area at different depths.

The Garmin specifications for the NMEA - 0183 sonar instrument lists the beam angle as 17.5 degrees. The linear coverage of this angle at depth is determined with the equation:

$$\text{Linear coverage (ft)} = 2 \cdot D \cdot \tan (a/2)$$

Where D = Depth in feet, and a = Beam width in degrees

Solution: Calculating linear coverage for each depth and converting to metric units produces the following beam width coverage for each depth (Figure 23).

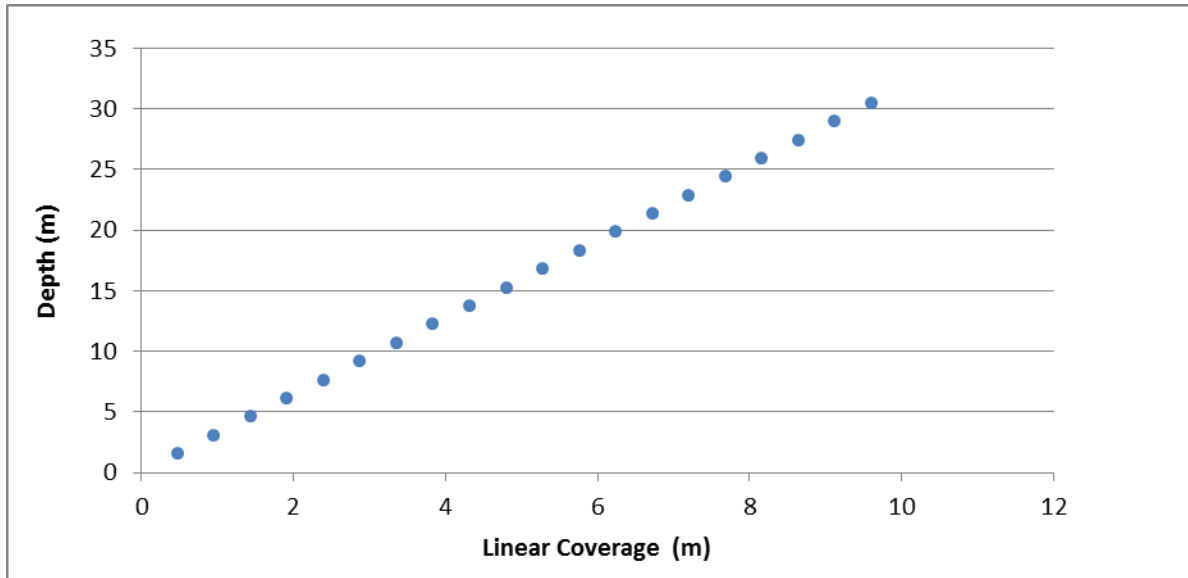


Figure 23. Linear coverage of sonar at depths from 1.5 to 30 m.

Test 8: Offset between the sonar-recorded point on the seafloor and surface instrument location.

The point at which the sonar beam intersects the seafloor will be within the area determined for that depth. At our deepest working depth (free diving depth) of 10 m, a 3 m wide area is ensonified¹. Only the shallowest point is recorded, which may be anywhere within that area. However, in low-relief sea floor substrates, objects in the center of the ensonified area are a shorter distance from the transducer and will produce the first returns. In high relief substrates, objects at the perimeter of the ensonified area may produce the quickest return, creating ± 1.5 m position offset from vertical center. To minimize this error, transects are run perpendicular to the contemporary shoreline to produce a better profile of submerged features that are likely parallel to shore.

Solution: The position recorded for the shallowest feature may be anywhere within the ensonified area. In deeper water, a larger area is ensonified and in high relief substrates, the edges of the ensonified area may be recorded. In both cases a position offset error may occur.

¹ To fill the ocean or any fluid medium with acoustic radiation which is then observed and analyzed to study the medium or to locate or image objects within it (Geller 2003).

Test 9: Depth variance due to surface disturbance.

High frequency transducers (100 kHz – 1000 kHz) are more precise for shallow water applications because high frequencies have shorter wavelengths, which allow the detection of smaller targets. A wider beam ($>8^\circ$) will be affected less by yaw, pitch and roll because of the greater coverage area directly below the transducer.

To determine the variance in depth due to changes in sea state, the transducer is held at different angles over a level surface with a known depth. The angle at which the transducer records a variance in depth is the point at which the vertical target is no longer ensonified. The US Army Corps of Engineers considers conditions with more than a 10 degree pitch or roll will produce an error of more than ± 0.06 m that is unacceptable for single beam sonar survey work. To produce results within this range of error, our instrument was tested by recording the depth measurement over a level surface at 5 and 10 degrees of roll and pitch using a level and angle measuring device (Table 11).

Table 11. Acoustic depth measurement with a 5 degree and 10 degree roll angle.

ADc (m)	MD (m)	Angle °
1.6	1.1	5
1.4	1.1	5
1.5	1.1	5
1.4	1.1	5
1.3	1.1	5
1.2	1.1	5
1.5	1.1	5
1.6	1.1	5
0.9	1.1	10
1.1	1.1	10
0.9	1.1	10
1.2	1.1	10
1.2	1.1	10
1.1	1.1	10
1.3	1.1	10
1.2	1.1	10

Statistical analysis of the pitch and roll test reveals that the average acoustic depth reading with a 5 degree angle at a depth of 1.1 m is 1.4 ± 0.14 m with a CV of 9.8%. For a 10 degree angle at the same depth the average depth reading is 1.1 ± 0.15 m with a CV of 13.1 % (Table 12).

A one sample analysis compares the average acoustic depth reading to the measured depth at 1.1 m at a 5 and 10 degree roll. At 5 degrees there is a statistically significant difference between the acoustic and measured average depth, $p = 0.0003$. However at 10 degrees the difference between the average depths is not significant, $p = 0.82$. This is problematic because we would expect the 10 degree angle to produce measurements further from the measured depth and result in a lower p value, and the opposite to be true for the 5 degree angle.

The paired means comparison reveals that the difference between the average measurements of the two angles is significant, $p = 0.0047$ which is expected due to the greater error expected at greater angles.

Table 12. Statistical analysis of acoustic depth measurement at 5 and 10 degree roll angle (respectively).

	Acoustic depth		Acoustic depth
Mean	1.438	Mean	1.113
Std. Dev.	.141	Std. Dev.	.146
Count	8	Count	8
Minimum	1.200	Minimum	.900
Maximum	1.600	Maximum	1.300
Coef. Var.	.098	Coef. Var.	.131
Range	.400	Range	.400
Median	1.450	Mode	1.200

One Sample Analysis
Hypothesized Mean = 1.1

	Mean	DF	t-Value	P-Value	95% Lower	95% Upper
Acoustic depth 5 degrees	1.438	7	6.780	.0003	1.320	1.555
Acoustic depth 10 degrees	1.113	7	.243	.8153	.991	1.234

Paired Means Comparison
Hypothesized Difference = 0

	Mean Diff.	DF	t-Value	P-Value	95% Lower	95% Upper
Acoustic depth 5 degrees, Acoustic depth 10 degrees	.325	7	4.082	.0047	.137	.513

Solution: Without a detection device for measurement and correction of yaw, pitch and roll, the best approach to reducing this error is to carefully select the conditions in which surveys are conducted. The major error is heave caused by wave height. Under calm conditions, the wave height and period should not exceed an error of ± 0.06 m. Wave height and period can be used to determine the heave error by using a stadia rod positioned vertically in shallow water (up to 3 m depth) and directly measuring the difference of the platform height for a few minutes. This will determine the maximum heave for those conditions. Repeating this test several times during the survey allows correction for heave. Pitch and roll are less of an issue because the sonar beam is wide and only records the seafloor point at the shortest angle. This means that the area directly beneath the transducer is recorded. However, in extremely shallow water (<3 m) the beam width of the sonar is narrow (<1 m), and the entire area ensonified may not be directly below the instrument, so surface motion will have a more dramatic effect on the point recorded. It is imperative to have absolutely calm conditions when surveying shallow areas. In deeper water, the effect of surface motion will have less of an impact on the point depth measurement.

Note: All testing was performed at the Hawaii Acoustic Tank (HAT) at Snugg Harbor, a facility of the Hydroacoustic Engineering And Research (HEAR) Laboratory. Comparative testing was performed at the enclosed lagoon area of Waikiki Beach. The depth range for this testing was limited to the depth of the HEAR lab tank which is 1.5 m. Testing in the Waikiki lagoon was also depth limited to 1.5 m. When calm ocean conditions are available, these same tests should be conducted in the full range of depths expected in the field at Papadiokampos (up to 30 m), to determine the expected performance of the instrument at these depths.

INSTRUMENT SPECIFICATIONS

Turbidity:

Model: 2020 LaMotte 1799 Turbidity Meter
Unit of Measure: NTU, FNU, FAU, ASBC, EBC
Range: 0-4000
Resolution: 0.01 NTU/FNU 0.00-10.99
0.1 NTU/FNU 11.00-109.9
1 NTU/FNU 110-4000
Accuracy: $\pm 2\%$ 0-100 NTU
 $\pm 3\%$ above 100 NTU
Detection Limit: 0.05 NTU/FNU
Reproducibility: 0.02 NTU/FNU
0.5 FAU
Calibration: AMCO standards of 1.00 NTU and 10.0 NTU

Salinity:

Model: VitalSine SR-6
Range: Salinity: 0-100%, Specific Gravity: 1.000-1.070
Resolution: Salinity: 1%, Specific Gravity: 0.001
Accuracy: Salinity: $\pm 1\%$, Specific Gravity: ± 0.001
Temperature Range: 10-30°C

Temperature:

Model: H22PX Hawkeye handheld depth finder with temperature
Units of Measure: feet & meters, Fahrenheit & Celsius
Depth Range - Max: 61 m
Depth Range - Min: 0.7 m
Depth Readout Increments: 0.1 m
Accuracy: $\pm 5\%$
Waterproof Rating: IP 8 (continuous submersion)
Temperature Range: -18 to 50 C
Sonar Frequency: 200 kHz
Transducer Beam Angle: 25 degrees
Temperature accuracy: $1/10^{\text{th}}$ degree for C or F

Sonar:

Model: Garmin Transom Mount Intelliducer
NMEA 0183-compatible
Temperature Range: -15°C to 33°C
Power: 150 W (RMS), 1,200 W (peak-to-peak)
Frequency: 160 kHz
Depth range: 0.9 - 275 m
sonar beam angle: 17.5 degrees
Depth accuracy: ± 10 cm at 0.90-10 m depth, ± 1 m at > 10 m depth

GPS:

Model: GPSMAP 76Cx
Receiver: WAAS/EGNOS enabled
Accuracy: 3-5 m
Interfaces: NMEA 0183 version 2.3, and RS-232 and USB for PC
Data Transfer: Power/Data serial port cable with bare wire leads

Camera:

Model: GoPro Hero+3 Black Edition with housing
Resolution: 12 MP
Lens: 6-element aspherical glass
Aperture: Fixed f/2.8 aperture

BIBLIOGRAPHY

- Andersen, H.-E., T. Clarkin, K. Winterberger and J. Strunk (2009) An accuracy assessment of positions obtained using survey and recreational grade global positioning system receivers across a range of forest conditions within the Tanana Valley of interior Alaska. *Western Journal of Applied Forestry*, 24, 128-136.
- Anzidei, M., F. Antonioli, A. Benini, K. Lambeck, D. Sivan, E. Serpelloni and P. Stocchi (2011) Sea level change and vertical land movements since the last two millennia along the coasts of southwestern Turkey and Israel. *Quaternary International*, 232, 13-20.
- Basu, A. and N. K. Saxena (1999) A review of shallow-water mapping systems. *Marine Geodesy*, 22, 249-257.
- Bormann, H., F. Ahlhorn and T. Klenke (2012) Adaptation of water management to regional climate change in a coastal region - Hydrological change vs. community perception and strategies. *Journal of Hydrology*, 454, 64-75.
- Boulton, S. J. and I. S. Stewart (2011) Holocene coastal notches in the Mediterranean: Palaeoseismic or Palaeoclimatic indicators? 2nd INQUA-IGCP-567 International Workshop on Active Tectonics, Earthquake Geology, Archaeology and Engineering, 1-3.
- Cazenave, A., C. Cabanes, K. Dominh and S. Mangiarotti (2001) Recent sea level change in the Mediterranean Sea revealed by Topex/Poseidon satellite altimetry. *Geophysical Research Letters*, 28, 1607-1610.
- Chen, C.-T. and F. J. Millero (1977) Speed of sound in seawater at high pressures. *Journal of Acoustic Society of America*, 62, 1129-1135.
- Collina-Girard, J. (2002) Underwater mapping of Late Quaternary submerged shorelines in the Western Mediterranean Sea and the Caribbean Sea. *Quaternary International*, 92, 63-72.
- Cooper, F. J., G. P. Roberts and C. J. Underwood (2007) A comparison of 103–105 year uplift rates on the South Alkyonides Fault, central Greece: Holocene climate stability and the formation of coastal notches. *Geophysical Research Letters* 34, L14310.
- Cundy, A. B., D. Sprague, L. Hopkinson, H. Maroukian, K. Gaki-Papanastassiou, D. Papanastassiou and M. R. Frogley (2006) Geochemical and stratigraphic indicators of late Holocene coastal evolution in the Gythio area, southern Peloponnese, Greece. *Marine Geology*, 230, 161–177.
- Dasgupta, S., A. K. Gosain, S. Rao, S. Roy and M. Sarraf (2013) A megacity in a changing climate: the case of Kolkata. *Climatic Change*, 116, 747-766.
- Desruelles, S., É. Fouache, A. Ciner, R. Dalongeville, K. Pavlopoulos, E. Kosun, Y. Coquinot and J.-L. Potdevin (2009) Beachrocks and sea level changes since Middle Holocene: Comparison between the insular group of Mykonos–Delos–Rhenia (Cyclades, Greece) and the southern coast of Turkey. *Global and Planetary Change*, 66, 19–33.
- DigitalGlobe (2011) Worldview 2 satellite 8-band imagery.
- Engel, M., M. Knipping, H. Brückner, M. Kiderlen and J. C. Kraft (2009) Reconstructing middle to late Holocene palaeogeographies of the lower Messenian plain (southwestern Peloponnese, Greece): Coastline migration, vegetation history and sea level Palaeogeography, Palaeoclimatology, Palaeoecology 284, 257-270.
- Evelpidou, N., K. Pavlopoulos, A. Vassilopoulos, M. Triantaphyllou, K. Vouvalidis and G. Syrides (2011a) Holocene palaeogeographical reconstruction of the western part of Naxos island (Greece). *Quaternary International*, 1-13.

- Evelpidou, N., P. A. Pirazzoli, J.-F. Sali and A. Vassilopoulos (2011b) Submerged notches and doline sediments as evidence for Holocene subsidence. *Continental Shelf Research*, 31, 1273–1281.
- FGDC (1998) Geospatial positioning accuracy standards.
- Freitas, R., A. M. Rodrigues, E. Morris, J. L. Perez-Llorens and V. Quintino (2008) Single-beam acoustic ground discrimination of shallow water habitats: 50 kHz or 200 kHz frequency survey? *Estuarine, Coastal and Shelf Science*, 78, 613-622.
- Gaki-Papanastassiou, K., E. Karymbalis, D. Papanastassiou and H. Maroukian (2009) Quaternary marine terraces as indicators of neotectonic activity of the Ierapetra normal fault SE Crete (Greece). *Geomorphology*, 104, 38–46.
- Gehrels, R. (2010) Sea-level changes since the Last Glacial Maximum: an appraisal of the IPCC Fourth Assessment Report. *Journal of Quaternary Science*, 25, 26-38.
- Geller, E. (2003) McGraw-Hill dictionary of scientific and technical terms.
- Gewelt, M. and G. Fierro (1983) The beach-rock of Capo Noli (Finale Ligure, Italy): 14C dating and diurnal variations of pH in pools. *Proceedings of the Orient House*, 8, 55-66.
- Giorgi, F. and L. Piero (2008) Climate change projections for the Mediterranean region. *Global and Planetary Change*, 63, 90–104.
- Goiran, J.-P. and C. Morhange (2003) Géographie des ports antiques de méditerranée. *Topoi* 11, 645–667.
- Goiran, J.-P., K. P. Pavlopoulos, E. Fouache, M. Triantaphyllou and R. Etienne (2011) Piraeus, the ancient island of Athens: Evidence from Holocene sediments and historical archives. *Geology*, 39, 531-534.
- Greenwalt, C. R. and M. E. Schultz (1968) Principles and error theory and cartographic applications. ACIC Technical 89.
- Guenther, G. C. (2007) Airborne Lidar Bathymetry, Digital Elevation Model Technologies and Applications: The DEM Users Manual, 2nd Edition.
- Guenther, G. C., A. G. Cunningham, P. E. LaRocque and D. J. Reid (2000) Meeting the accuracy challenge in airborne LiDAR bathymetry. *Proceedings of EARSeL-SIG-Workshop LIDAR*, 1-27.
- Guidoboni, E. and A. Comastri (1997) The large earthquake of 8 August 1303 in Crete: seismic scenario and tsunami in the Mediterranean area. *Journal of Seismology*, 1, 55-72.
- Hall, J. B. C., USN (2000) Principles of Naval Weapons Systems.
- IPCC (2013) Twelfth Session of Working Group I. Intergovernmental Panel on Climate Change.
- Jin, J. J. and H. Francisco (2013) Sea-level rise adaptation measures in local communities of Zhejiang Province, China. *Ocean & Coastal Management*, 71, 187-194.
- Kagan, Y. Y. and D. D. Jackson (2000) Probabilistic forecasting of earthquakes. *Geophysical Journal International*, 143, 438-453.
- Kenny, A. J. and I. Sotheran (2013) Methods for the Study of Marine Benthos, Characterising the Physical Properties of Seabed Habitats. Fourth Edition.
- Kershaw, S. and L. Guo (2001) Marine notches in coastal cliffs: Indicators of relative sea level change Perachora Peninsula, central Greece. *Marine Geology*, 179, 213–228.
- Lagares, F. (2007) Bathymetrical profiles in northern Croatia: Index of sea-level pauses in the Holocene. *Océanographie (Géologie Marine)*, 340, 49–56.

- Lambeck, K. (1995) Late Pleistocene and Holocene sea-level change in Greece and southwestern Turkey: a separation of eustatic, isostatic and tectonic contributions. *Geophysics Journal International*, 122, 1022-1044.
- Lambeck, K. and A. Purcell (2005) Sea-level change in the Mediterranean Sea since the LGM: predictions for tectonically stable areas. *Quaternary Science Reviews*, 24, 1969-1988.
- Lanbo, L. (2006) Wave propagation fundamentals: from energy point of view, energy partitioning at interfaces.
- Lykousis, V. (In Press) Sea-level changes and shelf break prograding sequences during the last 400 ka in the Aegean margins: Subsidence rates and palaeogeographic implications. *Continental Shelf Research*, 1-8.
- MacGillivray, J. A., L. H. Sackett and J. Driessen (1984) An Archaeological Survey of the Roussolakkos Area at Palaikastro. 79.
- Manoj, C., A. V. Kuvshinov, S. Maus and H. Luhr (2006) Ocean circulation generated magnetic signals. *Earth, Planets, Space*, 58, 429-439.
- Marcos, M. and M. N. Tsimplis (2008) Comparison of results of AOGCMs in the Mediterranean Sea during the 21st century. *Journal of Geophysical Research: Oceans*, 113, C12028.
- Marcos, M., M. N. Tsimplis and A. G. P. Shaw (2009) Sea level extremes in southern Europe. *Journal of Geophysical Research*, 114, C01007.
- Marriner, N. and C. Morhange (2007) Geoscience of ancient Mediterranean harbours. *Earth-Science Reviews*, 80, 137-194.
- Matheron, G. (1963) Principles of geostatistics. *Economic Geology* 58, 1246-1266.
- McClave, J. T. and T. Sincich (1997) *A First Course In Statistics*. 6th Edition, 519.
- Mitrovica, J. X. and W. R. Peltier (1991) On postglacial geoid subsidence over the equatorial oceans. *Journal of Geophysical Research: Solid Earth*, 96, 20053-20071.
- Morand, P., A. Kodio, N. Andrew, F. Sinaba, J. Lemoalle and C. Bene (2012) Vulnerability and adaptation of African rural populations to hydro-climate change: experience from fishing communities in the Inner Niger Delta (Mali). *Climatic Change*, 115, 463-483.
- Mourtzas, N. D. (2010) Sea level changes along the coasts of Kea island and paleogeographical coastal reconstruction of archaeological sites. *Bulletin of the Geological Society of Greece*, Proceedings of the 12th International Congress, 453-462.
- Mourtzas, N. D. (2012a) Archaeological indicators for sea level change and coastal neotectonic deformation: the submerged Roman fish tanks of the gulf of Matala, Crete, Greece. *Journal of Archaeological Science*, 39, 884-895.
- Mourtzas, N. D. (2012b) A palaeogeographic reconstruction of the seafront of the ancient city of Delos in relation to Upper Holocene sea level changes in the central Cyclades. *Quaternary International*, 250, 3-18.
- Mycoo, M. and A. Chadwick (2012) Adaptation to climate change: the coastal zone of Barbados. *Maritime Engineering*, 165, 159-168.
- NGS (1989) Geometric geodetic accuracy standards and specifications for using GPS relative positioning techniques. 5.0, 1-54.
- Niven, R. J. and D. K. Bardsley (2013) Planned retreat as a management response to coastal risk: a case study from the Fleurieu Peninsula, South Australia. *Regional Environmental Change*, 13, 193-209.
- NOAA (2013) NOAA Laboratory for Satellite Altimetry Sea Level Trends Map. 2013, Sea Level Trend Map 1993-2012.

- Norris, J. G., S. Wyllie-Echeverria, T. Mumford, A. Bailey and T. Turner (1997) Estimating basal area coverage of subtidal seagrass beds using underwater videography. *Aquatic Botany*, 58, 269-287.
- Peltier, W. R. (1999) Global sea level rise and glacial isostatic adjustment. *Global and Planetary Change*, 20, 93-123.
- Pirazzoli, P. A. (2005) A review of possible eustatic, isostatic and tectonic contributions in eight late-Holocene relative sea-level histories from the Mediterranean area. *Quaternary Science Reviews*, 24, 1989-2001.
- Rizos, C. and S. Han (2003) Reference station network based RTK systems-concepts and progress. *Wuhan University Journal of Natural Sciences*, 8, 566-574.
- Rona, P. A. (1995) Tectono-eustasy and Phanerozoic sea levels. *Journal of Coastal Research*, 17, 269-277.
- Rovere, A., M. Vacchi, M. Firpo and L. Carobene (2011) Underwater geomorphology of the rocky coastal tracts between Finale Ligure and Vado Ligure (western Liguria, NW Mediterranean Sea). *Quaternary International*, 232, 187-200.
- Rust, D. and S. Kershaw (2000) Holocene tectonic uplift patterns in northeastern Sicily: evidence from marine notches in coastal outcrops. *Marine Geology*, 167, 105-126.
- Scicchitano, G., F. Antonioli, E. F. C. Berlinghieri, A. Dutton and C. Monaco (2008) Submerged archaeological sites along the Ionian coast of southeastern Sicily (Italy) and implications for the Holocene relative sea-level change. *Quaternary Research*, 70, 26-39.
- Shahid, S. (2012) Vulnerability of the power sector of Bangladesh to climate change and extreme weather events. *Regional Environmental Change*, 12, 595-606.
- Shaw, B., J. A. Jackson, T. F. G. Higham, P. C. England and A. L. Thomas (2010) Radiometric dates of uplifted marine fauna in Greece: Implications for the interpretation of recent earthquake and tectonic histories using lithophilic dates. *Earth and Planetary Science Letters*, 297, 395-404.
- Shaw, J. W. (1990) Bronze Age Aegean harboursides. *Thera and the Aegean World III*, 1.
- Sivan, D. (2010) Millennial to decadal scale sea-level changes observed along the Mediterranean coast of Israel and their implications for the coastal areas. *RIMS News*, 9-12.
- Sivan, D., S. Wdowinski, K. Lambeck, E. Galili and A. Raban (2001) Holocene sea-level changes along the Mediterranean coast of Israel, based on archaeological observations and numerical model. *Palaeogeography, Palaeoclimatology, Palaeoecology*, 167, 101-117.
- Smith, C. J. and H. Rumohr (2013) *Methods for the Study of Marine Benthos, Imaging Techniques*. Fourth Edition.
- Sofianou, C. and T. Brogan (2009) The Excavation of House A.1 at Papadiokampos. *KENTRO*, 12, 6-9.
- Soles, J. S. (1983) A Bronze Age Quarry in Eastern Crete. *Journal of Field Archaeology*, 10, 33-46.
- Stewart, I. and C. Morhange (2009) *Coastal Geomorphology and Sea-Level Change. The Physical Geography of the Mediterranean*.
- Stirling, C. H. and M. B. Andersen (2009) Uranium-series dating of fossil coral reefs: Extending the sea-level record beyond the last glacial cycle. *Earth and Planetary Science Letters*, 284, 269-283.
- tenVeen, J. H. and P. T. Meijer (1998) Late Miocene to Recent tectonic evolution of Crete (Greece): geological observations and model analysis. *Tectonophysics*, 298, 191-208.

- UNEP (2012) Green Economy in a Blue World Synthesis Report. 2013.
- Urick, R. J. (1975) Principles of underwater sound. 2nd Edition.
- US Corp of Engineers (2002) Engineering and Design - Hydrographic Surveying. EM 1110-2-1003, Chapter 9, 1-46.
- USGS (1997) National Mapping Program Technical Instructions. Part 1 General - Standards for Digital Elevation Models, 1-17.
- USGS (2013) National Earthquake Information Center. 2013, Preliminary Determination of Epicenter data from 1973 to present.
- Vescogni, A., F. R. Bosellini, M. Reuter and T. C. Brachert (2008) Vermetid reefs and their use as palaeobathymetric markers: New insights from the Late Miocene of the Mediterranean (Southern Italy, Crete). *Palaeogeography, Palaeoclimatology, Palaeoecology*, 267, 89–101.
- Wachsmann, S. (1999) Seagoing ships & seamanship in the Bronze Age Levant. *International Journal of Nautical Archaeology*, 28, 200-206.
- White, N. J., J. A. Church and J. M. Gregory (2005) Coastal and global averaged sea level rise for 1950 to 2000. *Geophysical Research Letters*, 32, L01601.
- Wigley, T. M. L. and S. C. B. Raper (1987) Thermal expansion of sea water associated with global warming. *Nature*, 330, 127-131.
- Wong, G. S. K. and S. Zhu (1995) Speed of sound in seawater as a function of salinity, temperature and pressure. *Journal of Acoustic Society of America*, 97, 1732-1736.
- Woodworth, P. L. and R. Player (2003) The permanent service for mean sea level: an update to the 21st century. *Journal of Coastal Research*, 19, 287-295.